DOT-TST-75-141

DYNAMIC MODELLING FOR AUTOMOBILE ACCELERATION RESPONSE AND RIDE QUALITY OVER ROUGH ROADWAYS

ANTHONY J. HEALEY
CRAIG C. SMITH
RONALD O. STEARMAN
EDWARD NATHMAN

RESEARCH REPORT 14

DECEMBER 1974

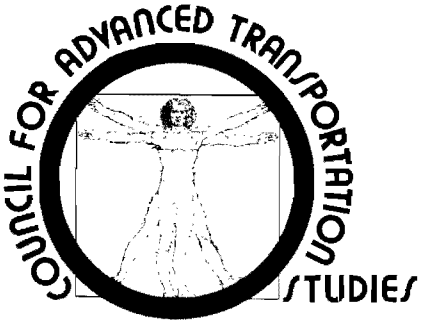

THE UNIVERSITY OF TEXAS AT AUSTIN

RESEARCH REPORTS PUBLISHED BY THE COUNCIL FOR ADVANCED TRANSPORTATION STUDIES

1 *An Integrated Methodology for Estimating Demand for Essential Services with an Application to Hospital Care.* Ronald Briggs, Wayne T. Enders, James Fitzsimmons, and Paul Jensen, April 1974 (DOT-TST-75-81).

2 *Transportation Impact Studies: A Review with Emphasis on Rural Areas.* Lidvard Skorpa, Richard Dodge, C. Michael Walton, and John Huddleston, October 1974 (DOT-TST-75-59).

3 *Land Value Modeling in Rural Communities.* Lidvard Skorpa, Richard Dodge, and C. Michael Walton, June 1974 (Draft Report).

4 *Inventory of Freight Transportation in the Southwest/Part I: Major Users of Transportation in the Dallas-Fort Worth Area.* Eugene Robinson, December 1973 (DOT-TST-75-29).

5 *Inventory of Freight Transportation in the Southwest/Part II: Motor Common Carrier Service in the Dallas-Fort Worth Area.* J. Bryan Adair and James S. Wilson, December 1973 (DOT-TST-75-30).

6 *Inventory of Freight Transportation in the Southwest/Part III: Air Freight Service in the Dallas-Fort Worth Area.* J. Bryan Adair, June 1974 (DOT-TST-75-31).

7 *Political Decision Processes, Transportation Investment and Changes in Urban Land Use: A Selective Bibliography with Particular Reference to Airports and Highways.* William D. Chipman, Harry P. Wolfe, and Pat Burnett, March 1974 (DOT-TST-75-28).

8 *A Preliminary Analysis of the Effects of the Dallas-Fort Worth Regional Airport on Surface Transportation and Land Use.* Harry P. Wolfe, April 1974 (Draft Report).

9 *Dissemination of Information to Increase Use of Austin Mass Transit: A Preliminary Study.* Gene Burd, October 1973.

10 *The University of Texas at Austin: A Campus Transportation Survey.* Sandra Rosenbloom, Jane Sentilles Greig, and Lawrence Sullivan Ross, August 1973.

11 *Carpool and Bus Matching Programs for The University of Texas at Austin.* Sandra Rosenbloom and Nancy Shelton Bauer, September 1974.

12 *A Pavement Design and Management System for Forest Service Roads: A Conceptual Study.* W. R. Hudson and Thomas G. McGarragh, July 1974.

13 *Measurement of Roadway Roughness and Motion Spectra for the Automobile Highway System.* Randall Bolding, Anthony Healey, and Ronald Stearman, December 1974 (DOT-TST-75-140).

14 *Dynamic Modelling for Automobile Acceleration Response and Ride Quality Over Rough Roadways.* Anthony Healey, Craig C. Smith, Ronald Stearman, and Edward Nathman, December 1974 (DOT-TST-75-141).

DYNAMIC MODELLING FOR AUTOMOBILE ACCELERATION RESPONSE AND RIDE QUALITY OVER ROUGH ROADWAYS

Anthony J. Healey
Craig C. Smith
Ronald O. Stearman
Edward Nathman

December 1974
RESEARCH REPORT

Prepared for

COUNCIL FOR ADVANCED TRANSPORTATION STUDIES
THE UNIVERSITY OF TEXAS AT AUSTIN
AUSTIN, TEXAS 78712

In cooperation with

DEPARTMENT OF TRANSPORTATION
OFFICE OF UNIVERSITY RESEARCH
WASHINGTON, D. C. 20590

NOTICE

This document is disseminated under the sponsorship of the Department of Transportation, Office of University Research, in the interest of information exchange. The United States Government, and the University of Texas assume no liability for its contents or use thereof.

Technical Report Documentation Page

1. Report No.	2. Government Accession No.	3. Recipient's Catalog No.
DOT-TST-75-141		

4. Title and Subtitle	5. Report Date
DYNAMIC MODELLING FOR AUTOMOBILE ACCELERATION RESPONSE AND RIDE QUALITY OVER ROUGH ROADWAYS	December 1974
	6. Performing Organization Code
7. Author(s) A.J. Healey, C.C. Smith, R.O. Stearman, and E. Nathman	8. Performing Organization Report No. RR 14
9. Performing Organization Name and Address Council for Advanced Transportation Studies The University of Texas at Austin Austin, Texas 78712	10. Work Unit No. (TRAIS) 00 3655 8 11. Contract or Grant No. DOT OS 30093
12. Sponsoring Agency Name and Address Department of Transportation Office of University Research Washington, D.C. 20590	13. Type of Report and Period Covered Research Report 14. Sponsoring Agency Code

15. Supplementary Notes

16. Abstract

Current interest in dynamics and vibration of ground transportation vehicles arises from the fact that excessive levels can lead to unsafe operation and give an uncomfortable ride to passengers.

Current work by the U.S. Dept. of Transportation in high-speed tracked air-cushion and magnetically levitated vehicles centers around suspension design (both active and passive) for isolating guideway roughness effects from the main body of the vehicle.

The work described herein arose from a need to evaluate vibration acceptance criteria for use in both vehicle systems design and guideway specification. This report deals with the first part of a study of automobile riding quality.

Three different models of an intermediate sedan together with two different models for roadway roughness are compared. Roadway models compared are, first, a random input single track model with statistics governed by a power spectral density proportional to the square of the wavelength and, second, a model using a data sequence with a zero order hold where the data sequence is obtained from measured evaluation profiles of actual roadway sections.

Frequency weighted rms acceleration responses are compared with servicability indices of roadway test sections.

17. Key Words	18. Distribution Statement
Ride Quality, Automobile, Response, Vibrations, Road, Roughness.	Document is available to the public through the National Technical Information Service, Springfield, Virginia 22151

19. Security Classif. (of this report)	20. Security Classif. (of this page)	21. No. of Pages	22. Price
Unclassified	Unclassified	52	

EXECUTIVE SUMMARY

INTRODUCTION

Current interest in dynamics and vibration of ground transportation vehicles arises from the fact that excessive levels can lead to unsafe operation and give an uncomfortable ride to passengers.

Current work by the U.S. Department of Transportation in high-speed tracked air-cushion and magnetically levitated vehicles centers around suspension design (both active and passive) for isolating guideway roughness effects from the main body of the vehicle.

The work described herein arose from a need to evaluate vibration acceptance criteria for use in both vehicle systems design and guideway specification. This report deals with the first part of a study of automobile riding quality.

Three different models of an intermediate sedan together with two different models for roadway roughness are compared. Roadway models compared are, first, a random input single track model with statistics governed by a power spectral density proportional to the square of the wavelength and, second, a model using a data sequence with a zero order hold where the data sequence is obtained from measured evaluation profiles of actual roadway sections.

Frequency weighted rms acceleration responses are compared with serviceability indices of roadway test sections.

It is concluded that the commonly used roadway model is inadequate and that more complete roadway information regarding statistics of right and left wheel tracks, together with a vehicle model including body roll motions, is necessary to predict ride quality.

Use of the ISO Standard on Whole Body Vibration Tolerances as a basis of frequency weighting provides a good correlation with subjective response measured in terms of the roadway servicability index.

RESULTS

As a result of the work it is shown that commonly used roughness models do not agree with experimentally obtained road roughness measurements. This means that discrepancies in predicted vibration levels can occur, making vehicle ride quality design uncertain.

Different models of a typical sedan automobile have been compared. It is shown that while the major motions of body heave, pitch, and wheel bounce are of primary importance, up to 15% error can be introduced in rms acceleration response when roll motions are neglected.

Roadway serviceability index is introduced here following work done in the pavement rating area. The serviceability index is a number on a 0-5 scale which represents the average feeling of a group of pavement raters about the acceptability of a particular stretch of roadway pavement. The serviceability index has been related to pavement roughness amplitude contents through regression analysis. It is thus possible to derive a serviceability index from knowledge of pavement roughness. This work has used the serviceability concept to explore the relationship between expected vibration levels (rms) and the serviceability index of a number of different roadways. The results show some scatter in the predictions but, generally, interstate quality roadways (SI range 4-5) yield vertical accelerations of 0.015 g(rms) or less while secondary roads (SI range 2-3) yield rms accelerations of between 0.045 g and 0.06 g. Trade-off curves are given relating vertical rms acceleration at the vehicle CG and at the driver's seat location to roadway serviceability.

UTILITY

The results are expected to be useful for those involved in the design of vehicle suspension systems and lend some insight toward the development of meaningful ride quality design criteria.

ABSTRACT

Current interest in dynamics and vibration of ground transportation vehicles arises from the fact that excessive levels can lead to unsafe operation and give an uncomfortable ride to passengers.

Current work by the U.S. Department of Transportation in high-speed tracked air-cushion and magnetically levitated vehicles centers around suspension design (both active and passive) for isolating guideway roughness effects from the main body of the vehicle.

The work described herein arose from a need to evaluate vibration acceptance criteria for use in both vehicle systems design and guideway specification. This report deals with the first part of a study of automobile riding quality.

Three different models of an intermediate sedan together with two different models for roadway roughness are compared. Roadway models compared are, first, a random input single track model with statistics governed by a power spectral density proportional to the square of the wavelength and, second, a model using a data sequence with a zero order hold where the data sequence is obtained from measured evaluation profiles of actual roadway sections.

Frequency weighted rms acceleration responses are compared with serviceability indices of roadway test sections.

It is concluded that the commonly used roadway model is inadequate and that more complete roadway information regarding statistics of right and left wheel tracks, together with a vehicle model including body roll motions, is necessary to predict ride quality.

Use of the ISO Standard on Whole Body Vibration Tolerances as a basis of frequency weighting provides a good correlation with subjective response measured in terms of the roadway servicability index.

ACKNOWLEDGMENTS

We gratefully acknowledge the support of DOT Contract No. DOT-OS-30093 administered through the Council for Advanced Transportation Studies at The University of Texas at Austin.

In addition we acknowledge the help of the NASA Langley Research Center, for the loan of the portable accelerometers, and the support of the Texas Highway Department and The University of Texas Center for Highway Research in the conduct of this project.

Table of Contents

NOMENCLATURE

z	= vertical displacement of the body	(in)
u	= vertical velocity of the body	(in/sec)
θ	= roll displacement of the body	(radians)
r	= roll velocity of the body	(radians/sec)
Φ	= pitch displacement of the body	(radians)
p	= pitch velocity of the body	(radians/sec)
ζ	= rear axle vertical displacement	(in)
v	= rear axle vertical velocity	(in/sec)
ξ	= rear axle angular displacement	(radians)
q	= rear axle angular velocity	(radians/sec)
a_1	= left front wheel vertical displacement	(in)
s	= left front wheel vertical velocity	(in/sec)
a_2	= right front wheel vertical displacement	(in)
w	= right front wheel vertical velocity	(in/sec)
δ_1	= displacement of road under left front tire	(in)
δ_2	= displacement of road under right front tire	(in)
δ_3	= displacement of road under left rear tire	(in)
δ_4	= displacement of raod under right rear tire	(in)
MS	= sprung mass, including passengers.	(lb-sec^2/in)
MRU	= rear unsprung mass	(lb-sec^2/in)
MUF	= one-half of total front unsprung mass	(lb-sec^2/in)
ISX	= roll moment of inertia of sprung mass	(in-lb-sec^2)

ISY = pitch moment of inertia of sprung mass (in-lb-sec^2)

IRU = roll moment of inertia of rear unsprung mass (in-lb-sec^2)

KSF = front suspension spring constant (lb/in)

KSR = rear suspension spring constant (lb/in)

KFB = front anti-sway bar spring constant (in-lb/rad)

KTF = front tires spring constant (lb/in)

KTR = rear tires spring constant (lb/in)

CF = front suspension damping constant (lb-sec/in)

CR = rear suspension damping constant (lb-sec/in)

CTF = front tires damping constant (lb-sec/in)

CTR = rear tires damping constant (lb-sec/in)

ALL SUCEEDING DISTANCES ARE GIVEN IN INCHES

XFS = distance from C.G. to line between front spring/ damper units

XRS = distance from C.G. to line between rear coil springs

XRC = distance from C.G. to line between rear dampers

YFS = distance from longitudal axis to front spring/dampers

YFB = distance from longitudal axis to front body/sway bar mount

YRS = distance from longitudal axis to rear springs

YRC = distance from longitudal axis to rear dampers

YRB = distance from longitudal axis to rear body/sway bar mount

BF = distance from longitudal axis to front suspension pin joint

NT = length of front transverse suspension arm

NS = distance from body/suspension arm pin joint to front spring/damper unit

N_B = distance from body/suspension arm pin joint to anti sway bar/suspension arm joint

B_T = half length of rear axle

B_S = distance from center of rear axle to rear spring

B_C = distance from center of rear axle to rear damper

B_B = distance from center of rear axle to rear anti-sway bar/axle pin joint

R_F = moment arm of front anti-sway bar

R_R = moment arm of rear anti-sway bar

$$NKS = K_{SF}(N_S/N_T)2$$

$$NCC = C_F(N_S/N_T)^2$$

$$F1 = NCC + C_R$$

$$F2 = X_{FS}\ NCC - X_{RC}\ C_R$$

$$F3 = NKS + KSR$$

$$F4 = X_{FS}\ NKS - X_{RS}\ K_{SR}$$

$$F5 = C_F(Y_{FS}-B_F(1-N_S/N_T))^2 + C_R Y_{RC}^2$$

$$F6 = K_{SF}(Y_{FS}-B_F(1-N_S/N_T))^2 + 2(K_{FB}/R_F)(N_B + B_F N_B/N_T)^2 + K_{SR}Y_{RS}^2 + 2(K_{RB}/R_R)\ B_B^2$$

$$F7 = 2 B_B^2 K_{RB}/RR + B_S K_{SR} Y_{RS}$$

$$F8 = K_{SF}(Y_{FS} - B_F(1-N_S/N_T))\ N_S/N_T + 2 K_{FB}/R_F(N_B + B_F N_B/N_T)\ N_B/N_T$$

$$F9 = X_{RC}^2 C_R + X_{FS}^2 C_F (N_S/N_T)^2$$

$$F10 = X_{RS}^2 K_{SR} + X_{FS}^2 NKS$$

$$F11 = C_R + C_{TR}$$

$$F12 = K_{SR} + K_{TR}$$

$$F13 = B_T^2 C_{TR} + B_C^2 C_R$$

$$F14 = B_T^2 K_{TR} + B_S^2 K_{SR} + 2 B_B^2 K_{RB}/R_R$$

$$F15 = -((1-N_S/N_T) B_F - Y_{FS}) N_S C_F/N_T$$

$$F16 = C_{TF} + NCC$$

$$F17 = -K_{SF}((1-N_S/N_T)B_F - Y_{FS})\ N_S/N_T + 2(B_F N_B/N_T + N_B)\ K_{FB}N_B/(N_T R_F)$$

$$F18 = K_{TF} + NKS + (K_{FB}/R_F)(N_B/N_T)^2$$

$$F19 = C_F (Y_{FS} - B_F(1-N_S/N_T))N_S/N_T$$

$$F20 = (K_{FB}/R_F)(N_B/N_T)^2$$

List of Figures

CHAPTER 1. INTRODUCTION

Current interest in dynamics and vibration of ground transportation vehicles arises from the fact that excessive levels of these characteristics can lead to unsafe operation and cause uncomfortable rides for passengers.

Current work of the US Department of Transportation in high-speed tracked air-cushion (TACV) and magnetically levitated (MAGLEV) vehicles centers around suspension design (both active and passive) for isolating guideway roughness effects from the main body of the vehicle.

The work described herein arose from a need to evaluate vibration acceptance criteria for use in both vehicle systems design and guideway surface specification. This report presents the first part of a study dealing with automobile riding quality. Since automobile riding quality is generally acceptable to the large majority of users, this study is helpful in understanding the effects of roadway roughness on the vehicle vibrational levels over a generally acceptable (to a greater or lesser extent, depending on road condition) range. This will help in evaluating ride quality criteria for use with systems employing TACV, MAGLEV and PRT vehicles. Also, earlier work[1] dealing with acceptability of roadway pavements is extended herein to the vehicle motion responses expected with pavements of varying acceptability.

Earlier work by Clark[2] viewed the vehicle-roadway system from the point of view of the dynamic loads imposed on the highway. A four degree of freedom model was employed with an assumed harmonic road profile. Mitschke[3] employed a narrow band approach using a power spectral density model for the roughness and a four degree of freedom vehicle model. Again, four degrees of freedom were used for simplicity even though agreement between analysis and experiment was marginally

---

1 Walker, R. S. and Hudson, W. R., "The Use of Profile Wave Amplitude Estimates for Pavement Servicability Measures," Paper presented at 52nd Annual Meeting of the Highway Research Board, January 1973.

2 Clark, D. C., "A Preliminary Investigation into the Dynamic Behavior of Vehicles and Highways," SAE Transactions, Vol. 70, pp. 447-455, 1962.

3 Mitschke, M., "Influence of Road and Vehicle Dimensions on the Amplitude of Body Motions and Dynamic Wheel Loads (Theoretical and Experimental Vibration Investigations), SAE Transactions, Vol. 70, pp. 434-447, 1962.

acceptable. Kohr,[4] employed a seven degree of freedom model with deterministic triangular bumps with reasonable success in prediction of body displacement response but acceleration responses were less accurately predicted. More recent work with high-speed ground transportation models [5,6,7,8,9] has usually employed four degrees of freedom and a single profile statistically described by a simple equation for its power spectral composition.

The important difference between this and other studies of automobile dynamics[10,11,12] is that actual roadway roughness profiles are used. Right and left wheel-tracked roughnesses are allowed to be different, thus inducing vehicle roll motions, and the acceleration responses predicted using measured roughness profiles are compared with those obtained using more familiar analytical roughness models and reduced order vehicle models.

---

[4] Kohr, R. H., "Analysis and Simulation of Automobile Ride," SAE Transactions, Vol. 49, pp. 110-119, 1961.

[5] Vender, E. K. and Paul, I. L., "Analysis of Optimum and Preview Control of Active Vehicle Suspensions," PB-176-137, 1967.

[6] "Tracked Air Cushion Research Vehicle - Volume 1 Research Vehicle Preliminary Design" - Grumman Aircraft Engineering Corporation Final Report. Clearinghouse No. PB-183-172, 1969.

[7] Wilkie, D. F. and Borcherts, R. H., "Dynamics Characteristics and Control Requirements for Alternate Magnetic Levitations Systems," ASME Paper No. 73-ICT-17. Presented at 2nd ICT Denver, Colorado, September, 1973.

[8] Young, J. W. and Wormley, D. N., "Optimization of Linear Vehicle Suspensions Subject to Simultaneous Guideway and External Force Disturbances," Transactions of ASME, Journal of Dynamics Systems, Measurement and Control, Vol. 95, No. 2, pp. 213-219, June 1973.

[9] Katz, R. M., Nene, V. D., Ravera, R. J. and Skakki, C. A., "Performance of Magnetic Suspensions for High-Speed Vehicles Operating over Flexible Guideways," ASME Paper No. 73-ICT-89. Presented at 2nd Intersociety Transportation Conference, Denver, Colorado, ASME, United Engineering Center, New York, New York.

[10] Dailey, G., Caywood, W. C., and O'Connor, J. C., "A General Purpose Computer Program for the Dynamic Simulation of Vehicle - Guideway Interactions," AIAA Journal, Vol. 11, No. 3, pp. 278-282, 1973.

[11] Lins, W. F., "Vehicle Vibration Analysis Using Frequency Domain Techniques," Transactions of ASME Journal of Engineering for Industry, pp. 1075-1080, 1969.

[12] Sinha, B., "Influence of Road Unevenness on Road Holding and Ride Comfort," Report No. 1, 1972, Institutionen för Maskinelement, Fordonsteknik Tekniska Högskolan, Stockholm, 1972.

CHAPTER 2. ROADWAY ROUGHNESS MEASUREMENT

While a large area of discrete roughness such as a rut can be considered as a deterministic reduction in roadway elevation, the dominant roughness occurs as a random variation of elevation. The mean elevation is not important but the random variations about the mean for any given section of roadway give rise to the need to treat the surface stochastically. Significant measures of the profiles are the variance and the power density spectrum.

Roughness profiles were measured with a Surface Dynamics Profilometer[13] (Figure 1). This is basically a Chevrolet carry-all truck with two sensing wheels - one in each wheel track - which are spring loaded to contact the roadway surface. This enables the system to be used at high speed (up to 60 mph). The instrumentation used consisted of an accelerometer located on the truck body immediately over each sensing wheel and a potentiometer to measure relative displacement between body and sensing wheel. The system block diagram is shown in Figure 2. The accelerometer signal is twice integrated, summed with the potentiometer signal to extract absolute motion of the sensor wheels, band-pass filtered, and recorded on analog tape. A pulse generator connected to the vehicle transmission provides a distance count to eliminate speed variation effects in the data. An automatic speed control is provided for driver convenience. The sensor wheels are made concentric with their shafts to within 0.005" and a natural rubber tire is molded to the wheel rim.

In making profile measurements, the short wavelength roughness is sensed primarily by the sensor wheel because of the isolation characteristic of the suspension system. The long wavelengths arising from hills and valleys are sensed primarily by the accelerometers. The double integration of the acceleration signal thus saturates the tape recorder unless adequate high pass filtering is provided. Four filters can be selected, depending on wavelength range and vehicle speed. At a 20-mph measurement speed, for example, the filter used introduces a 3 dB attenuation at 0.6 rad/sec, corresponding to a 306-ft wavelength.

---

[13] Mitschke, M., "Influence of Road and Vehicle Dimensions on the Amplitude of Body Motions and Dynamic Wheel Loads (Theoretical and Experimental Vibration Investigations), SAE Transactions, Vol. 70, pp. 434-447, 1962.

Figure 1. Photograph of G. M. Surface Dynamics Profilometer

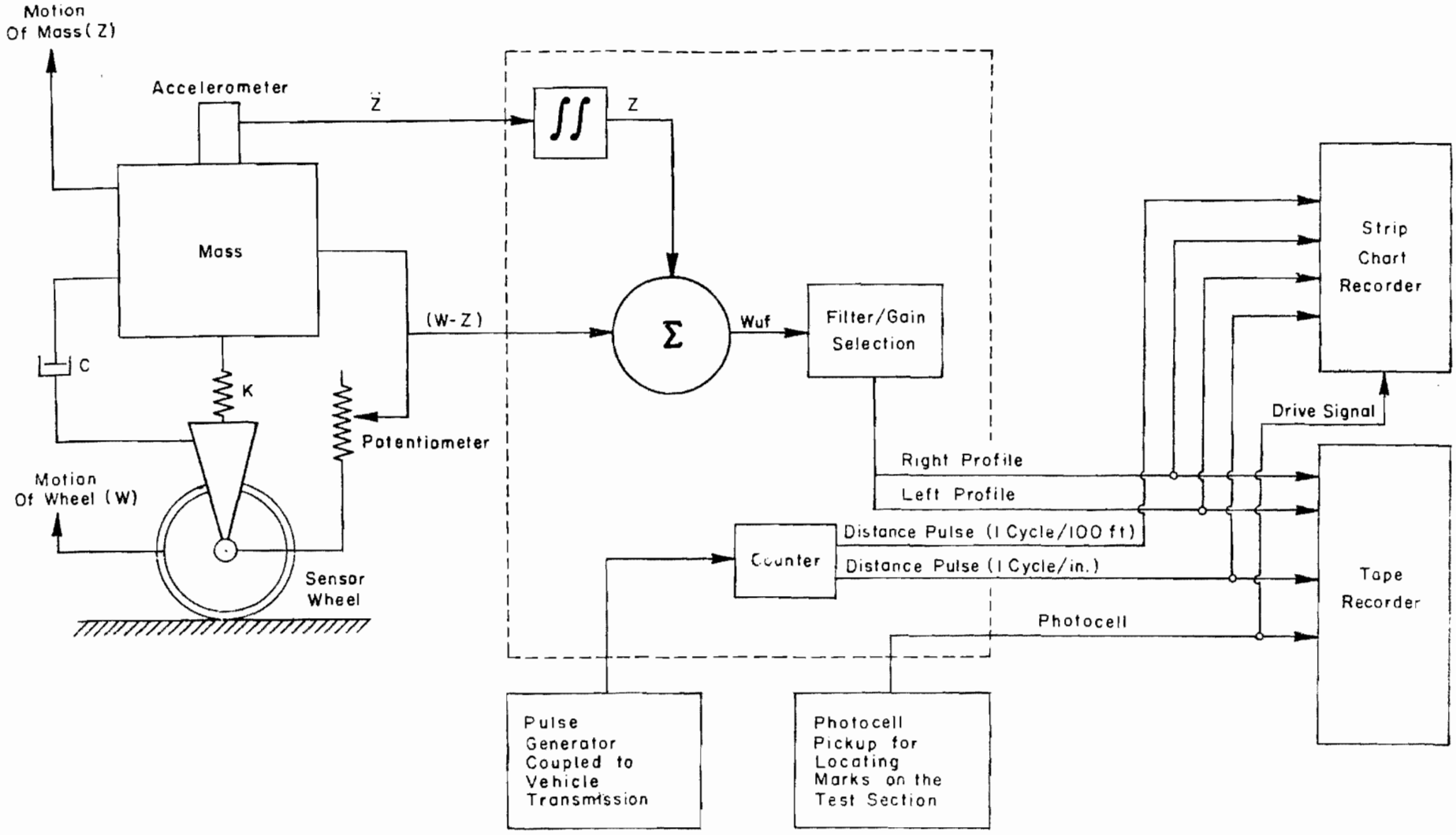

Figure 2. Profilometer Block Diagram

High frequency cut off occurs at 1000 rad/sec. Since the high-pass filter characteristic is known it may be compensated for in the data analysis.

The filtered profile together with pulser output and photocell pulses to denote beginning and end of a test section are recorded and subsequently digitized for analysis. The pulse generator output is fed to a counter which reduces the count to approximately 11.8 pulses per foot.

An H-P 2115A data processor is used for analog-to-digital conversion. Samples of right and left track are taken alternately, resulting in 5.9 samples per foot for each track. At the test speed of 20 mph, this is sufficient to prevent aliasing problems in the digitizing.

2.1 Data Analysis and Power Spectral Computations

The H-P 2115A processor produces 12-bit words written on digital tape in 1500 word blocks at 566 bpi. Data analysis is carried out on a CDC 6600 machine and a transformation program converts the H-P 5101 tape into CDC 6600 compatible data (60-bit words), ending with a sequence of right and left wheel track elevation data:

$$x_0, x_1, x_2, \ldots, x_n$$

$$y_0, y_1, y_2, \ldots, y_n$$

For each test section 4096 samples are taken, corresponding to a 694-ft record length. A segment of a typical trace is shown in Figure 3.

2.2 Detrending

The roadway statistics are assumed to be random, stationary, and ergodic. Because of the form of many test sections, not only the mean, but also the linear trend, is extracted in computing deviations. Detrending is accomplished by the operation

$$x_k = x_{old} - \bar{x} - \beta(k - \bar{k}) \qquad (1)$$

where $\bar{x}$, the mean, $= \frac{1}{N} \sum_{k=0}^{N-1} x_k$

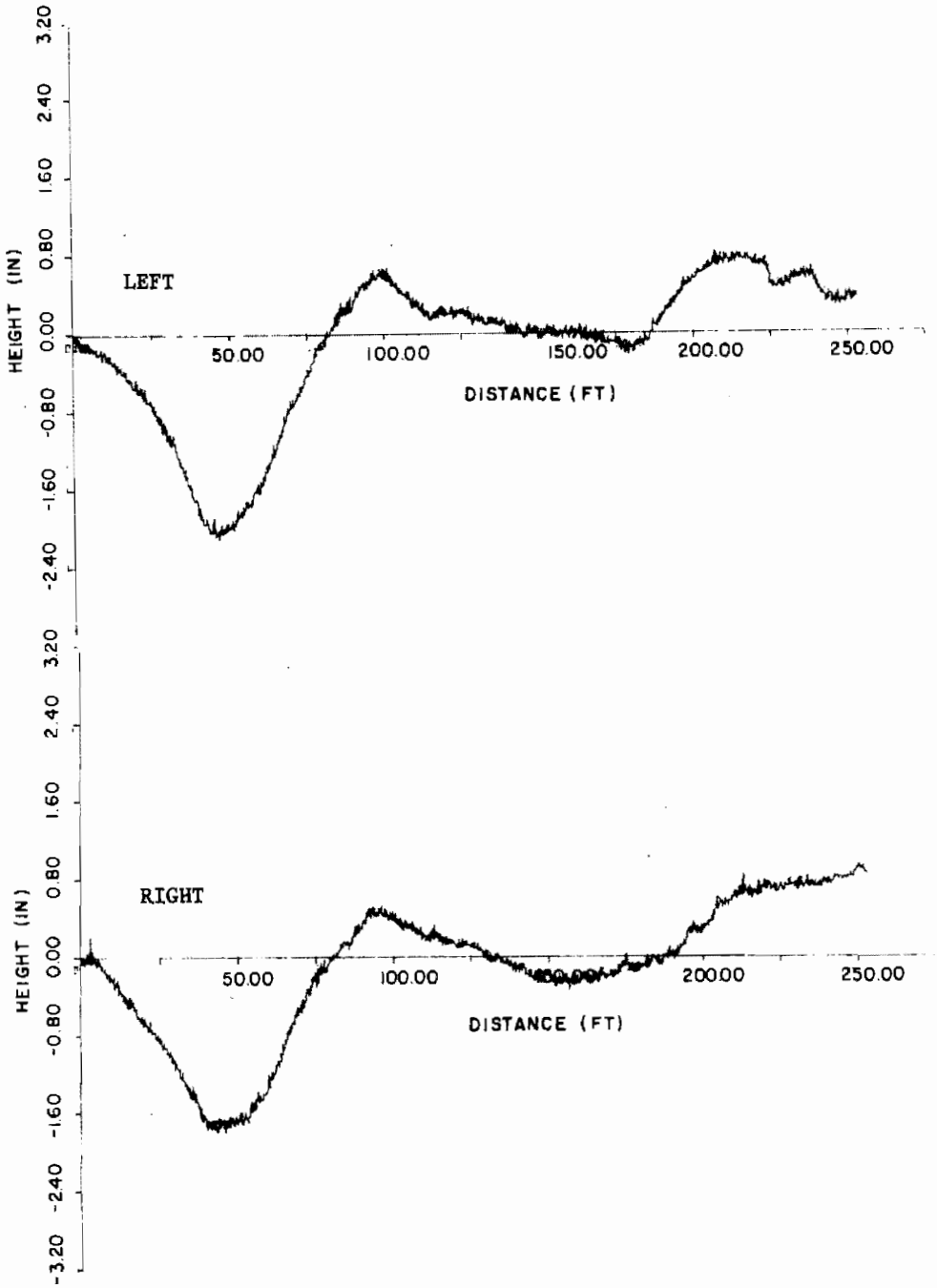

Figure 3. Typical Elevation Profile Plotted for Digitized Data (Texas Highway Department Section 6)

$$\bar{k} = \frac{1}{2}(N + 1)$$

and
$$\beta = \frac{\sum_{k=1}^{N} k x_{k-1} - \frac{1}{2} N(N+1)\bar{x}}{\frac{1}{6}N(N+1)(2N+1) - \frac{1}{4}N(N+1)^2}$$

The resulting sequence

$$(x_0 \ldots x_k \ldots x_{N-1})$$

is analyzed for its power spectral composition. The auto covariance is obtained by

$$C(r) = \frac{1}{N} \sum_{k=0}^{N-1} x_k \cdot x_{k+r} \qquad (2)$$

2.3 Power Spectrum Calculations

The power spectral density is then given by the discrete Fourier transform of C(r):

$$P(k) = \frac{1}{N} \sum_{r=0}^{N-1} C(r) e^{-j 2\pi rk/N} \qquad (3)$$

If the original sequence x_k is real, P(k) will be complex with a real and imaginary part being symmetric and anti-symmetric, respectively, about the N/2 point.

Taking advantage of the Fast Fourier Transform Algorithm[14], it is better to compute the FFT of x_k. Using the property that the transform of a convoluted sequence is the product of the individual transforms with it, conjugate so that if

$$X(k) = \frac{1}{N} \sum_{r=0}^{N-1} x_r e^{-j 2\pi rk/N} \qquad (4)$$

---

[14] Brigham, E. O. and Morrow, R. I., "The Fast Fourier Transform," IEEE Spectrum, Vol. 4, pp. 63-70, December, 1967.

the power density is

$$P(k) = (X_k X_k^*)\ L \tag{5}$$

where L = total record length, which is included to reconstitute dimensional units in the power function (L = 694 ft).

The leakage involved in reconstruction of finite data traces, which are inherently assumed to be periodic, are overcome by windowing. Here, a cosine taper window is employed, and a sufficient number of zeros are then added to the sequence to ensure that N is an integer power of two to provide compatability with the FFT algorithm.

The window used was

$$x_r = x_{old} \cdot W_r$$

$$W_r = \begin{cases} 0.5\ [1 - \cos\ (\pi(k' - 1/2)/r] & 1 < k < r \\ 1.0 & r < k < N - r \\ 0.5\ [1 - \cos\ [\ \pi(N - k + 1/2)/r]] & N - r < k < N \end{cases} \tag{6}$$

r was chosen as N/10

2.4 High Pass Filter Correction on Roadway PSD Calculations

The transfer function of the high-pass filter used in the profilometer measurements to avoid saturation of the recording equipment is

$$G_f(j\omega) = \frac{(\frac{j\omega}{\omega_n})^3}{(\frac{j\omega}{\omega_n})^3 + (1 = 2\zeta)(\frac{j\omega}{\omega_n})^2 + (1 + 2\zeta)(\frac{j\omega}{\omega_n}) + 1} \tag{7}$$

where $\zeta = 0.5$ for all filters and where ω_n can be chosen as 0.3, 0.6, or other values, depending upon the requirements of the particular roadway being measured. To correct the power density measurements for the high pass filter effect, each power spectra density is multiplied by the square of the magnitude of the filter transfer function at the appropriate frequency:

$$p_k^{corrected} = p_k^{filtered} \quad \frac{\cdot}{\cdot} \quad |G_f(j\omega_k)|^2 \tag{8}$$

where

$$\omega_k = \frac{2\pi k\ V_m}{L}$$

V_m = velocity of profilometer during profile measurement,

L = test section length.

2.5 Data Averaging

Because of the finite length of the measured trace and the nonstationarity of actual profiles, data averaging is necessary.

The sampling frequency occurred at about 5.9 cycles per foot and the incremental discretion frequency was 0.00144 cpf. Averaging over d incremental bands yielding d degrees of freedom for each averaged power computation, the power spectral sequence

$$P_o - - P_k - - P_n$$

converts to the data smoothed sequence

$$\hat{P}_d - - \hat{P}_k - - \hat{P}_{N-1-d}.$$

According to

$$\hat{P}_k = \frac{1}{(2d+1)} \sum_{k-d}^{k+d} P_k \ ; \ k = d \text{ to } N-1-d. \qquad (9)$$

The frequency associated with $\hat{P}_k$ still remains at k/L cycles/ft.

While equation (9) smoothes the data, total power is not conserved in the smoothing process. The errors are introduced by the failure to include points from k = 0 to d and k = (N - 1 - d) to k = (N - 1). With typical spectra this error is small. Total power error is given by

$$\text{Total Power Error} = \frac{1}{(2d+1)} \sum_{\lambda=0}^{\lambda=2d} (2d-\lambda)(P_\lambda + P_{N-1-\lambda})$$

A typical result for the averaged power density of a section of highway is shown in Figure 4. The abscissa has been converted to Hz rather than cycles per foot in view of our interest in ride quality. The conversion is

$$F(\text{cpf}) = \frac{f(\text{Hz})}{V(\text{fps})} \quad ; \text{ where } V = \text{test vehicle speed (in ft. per second)}$$

Figure 5 shows data for individual tracks for several rough, medium, and smooth roads while Figure 6 shows plots of cross power, where

$$\text{Cross Power} = L(X_k^* Y_k) \tag{10}$$

Cross-powers are complex quantities and Figure 6 shows plots of the magnitude of (10) of six test sections.

2.6 Discussion of Road Profile Measurements

Figure 5 shows the general nature of roadway random roughness power to be roughly inversely proportional to frequency squared. This conclusion had been reached earlier by Houboult[15] and is partially reconfirmed here. The major difficulty in using the assumption that

$$p(F) = A/\Omega^2 \ \text{in}^2/\text{cpf} \ . \quad \frac{AV}{f^2} \ \text{in}^2/\text{Hz} \tag{11}$$

lies in the variability of A. Figure 5 shows that the value of the effective A can vary from state route quality to interstate quality roads by a factor of 10. This could make a predicted ride acceleration magnitude based upon a standard value of A error by a factor of about three to one - a significant difference when it comes to ride quality analysis.

A detailed discussion of measured profiles appears in reference 16[16]. Therein it is shown that equation 11 is valid only within a narrow frequency

---

[15] Houboult, J. C., "Runway Roughness Studies in the Aeronautical Field," Transactions of ASCE, Vol. 127, Part IV, pp. 428-447, 1962.

[16] Bolding, R., Healey, A. J., and Stearman, R. O., "Measurement of Roadway Roughness and Vehicle Motion Spectra for the Automobile - Highway System," Research Report IV - 3, Council for Advanced Transportation Studies, The University of Texas at Austin, 1974.

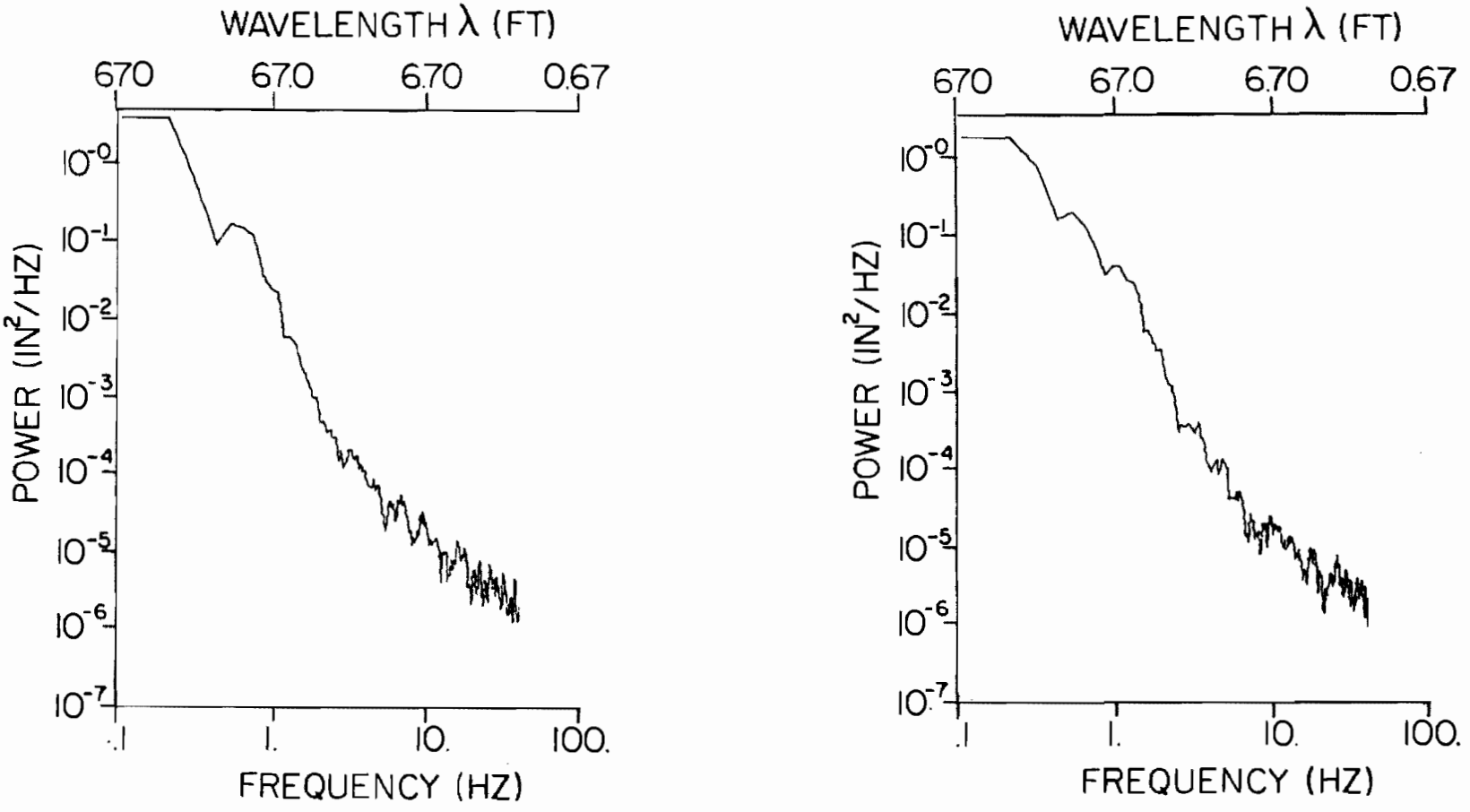

Figure 4. Averaged Power Spectral Density (in^2/Hz) Versus Temporal Frequency (Hz) at 50-mph Traverse Speed - THD Section 6

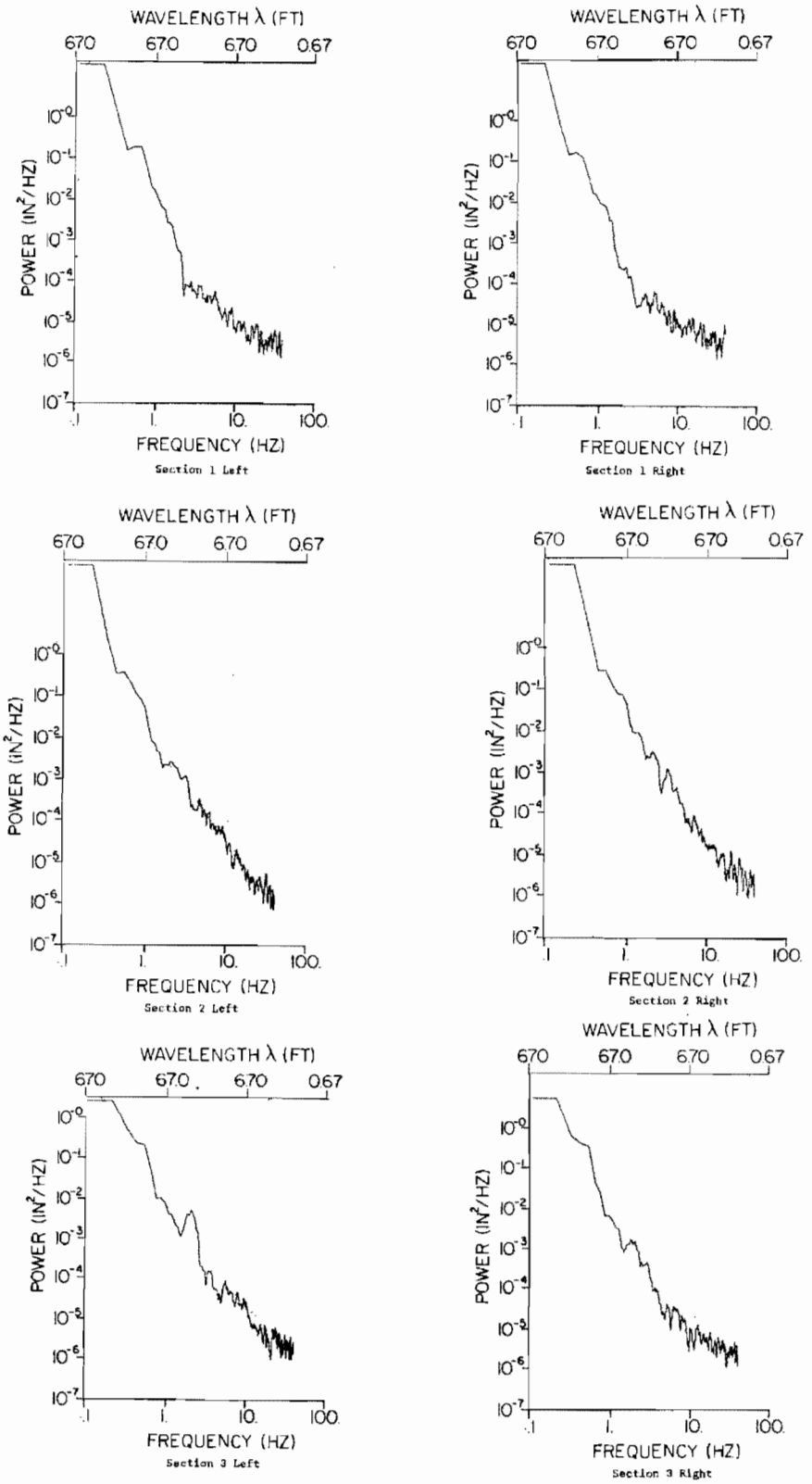

Figure 5. Elevation Power Spectra for Right and Left Tracks (in^2/Hz) Versus Temporal Frequency (Hz) at 50 mph

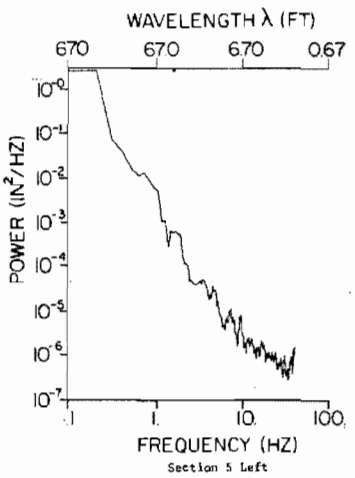

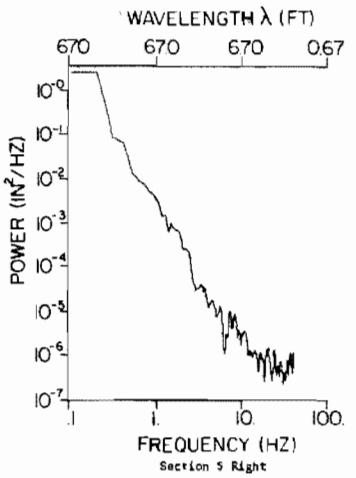

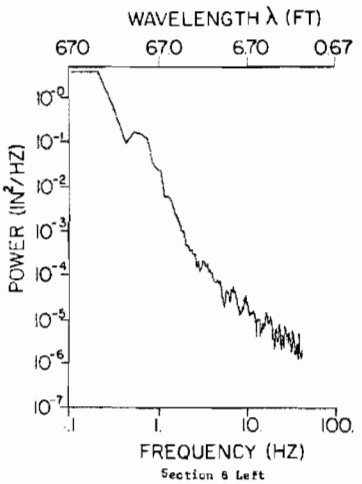

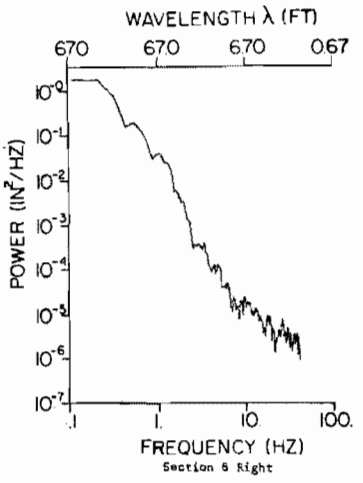

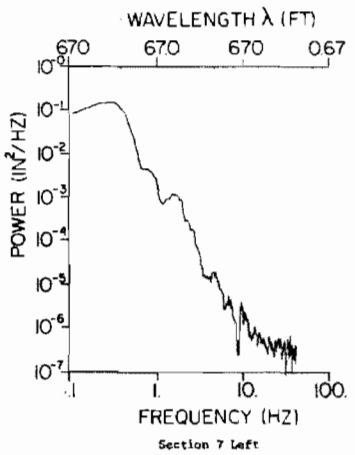

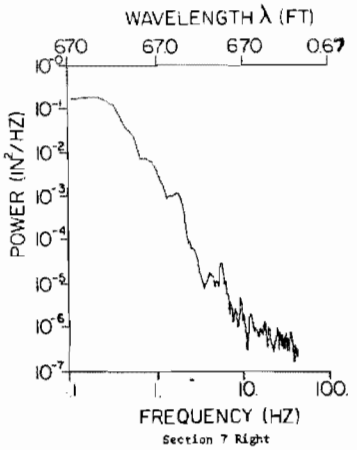

Figure 5. (continued)

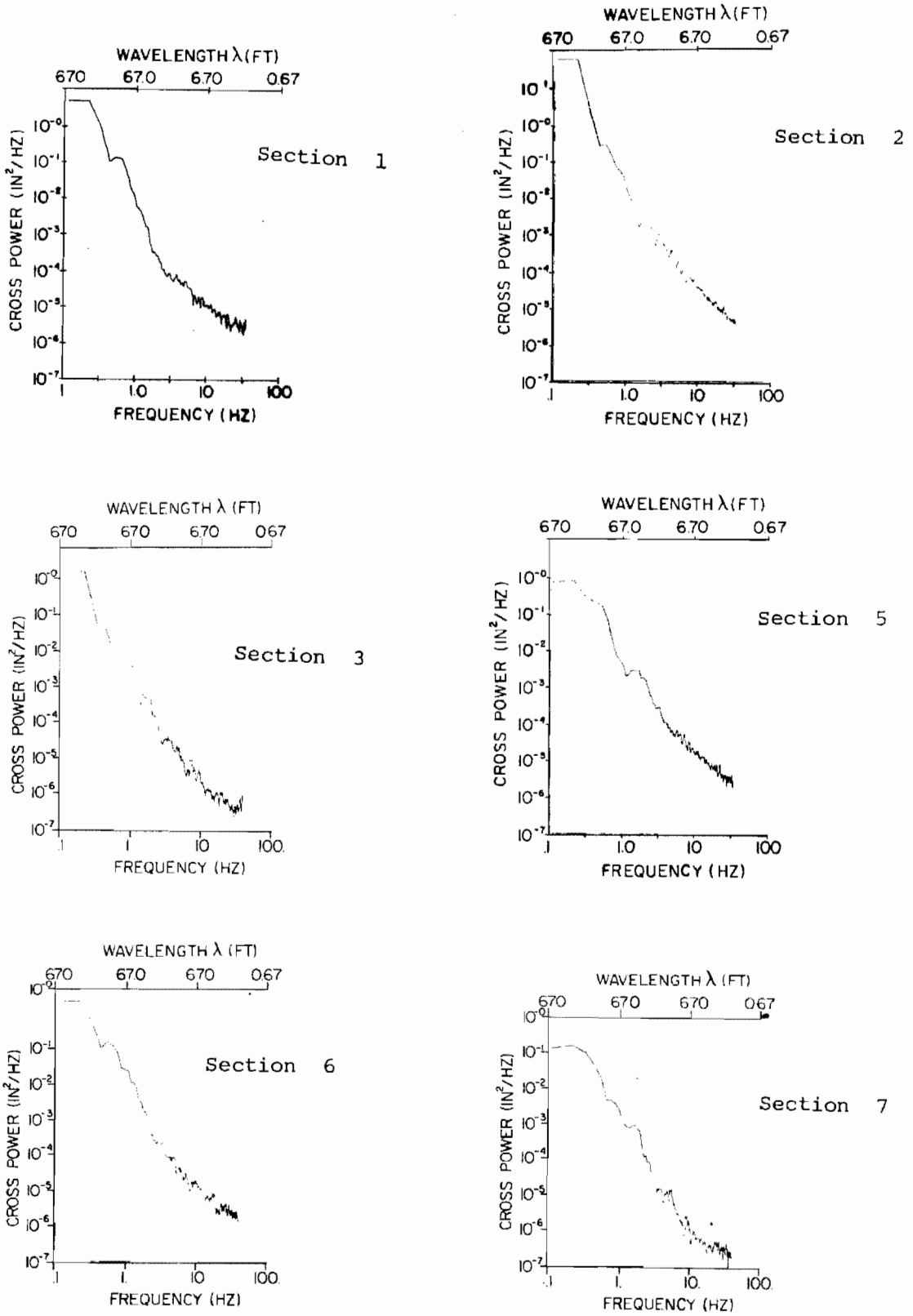

Figure 6. Magnitude of Elevation Cross-Power Between Right and Left Tracks (in^2/Hz) Versus Temporal Frequency (Hz) at 50 mph

range. A two segment description of roadway inputs has been proposed[17] although more detailed study is needed to determine its validity. The choice of an appropriate constant for A hinges on the frequency range of interest. For example, in ride quality work the range 0.1 Hz to 40 Hz is certainly of most significant interest. Equating mean square values of the ideal profile (equation 11) with a measured profile will yield a best fit A for the chosen range.

Integrating equation (11) over the 0.1 Hz to 40 Hz range yields the mean squared value

$$E(x^2) = (AV)(10) \text{ in}^2$$

Table I gives comparisons between measured $E(x^2)$ and best fit A for each section of Figure 5.

Comparing Figures 6 and and 5, it is seen that the magnitude of the cross-power spectral density is very similar to the direct powers of each individual

TABLE I

Section	RMS roughness (in.)	$A(in^2/ft)$
1	2.49712	8.503102×10^{-3}
2	4.95043	3.34183×10^{-2}
3	1.20441	1.978095×10^{-3}
5	0.766755	8.01699×10^{-4}
6	0.815170	9.061393×10^{-4}
7	0.267746	9.77563×10^{-5}

NOTE: To convert A into ft. units, divide by 144.0

profile. This suggests the assumption that $p_x = p_y = p_{xy}$. This has been proposed by Dodds and Robson[18]. Although convenient and simple its validity

[17] Dodds, C. J. and Robson, J. D., "The Description of Road Surface Roughness," Journal of Sound and Vibration, Vol. 31, Part 2, pp. 175-183, 1973.

[18] Ibid.

for our data has not been thoroughly examined. The assumption implies a real cross power and leads to the conclusion that right and left track roughness profiles are statistically identical. The effects of the simplification on vehicle ride quality are discussed later.

CHAPTER 3. VEHICLE DYNAMICS

In view of apparently significant cross-power phases between right and left wheel track profiles, a seven degree of freedom vehicle model was employed. The model represents a 1974 Buick Century with major parameters measured and the remainder calculated or estimated.

Right and left wheel tracks are allowed to be different. The effects of different track profiles are discussed later on in this report. The vehicle model treats the automobile body as rigid with three motion degrees of freedom, heave, pitch, and roll. The two front wheels are independently sprung and are assumed to move vertically, each contributing one independent wheel hop degree of freedom. Front suspensions are modeled as a spring and damper acting on a lever arm with an effective "tire and wheel lumped mass" on its extremity. The rear suspension incorporates a solid rear axle with leaf springs, dampers, and tires modeled as lumped components acting at their respective points of attachment. A mass distribution for the real axle was calculated as explained later in the discussion of model parameters. A sway bar, modeled for torsion and bending modes for compliance, was incorporated in the front suspension model. Provision was also made for inclusion of a rear sway bar if needed. Figure 7 shows a diagram of the components of the model. A "visco-elastic" model for pneumatic tire compression was chosen. Modeling the body as a rigidly sprung mass, it is assumed that passenger motions are induced by the body motions but that they do not in return dynamically modify the vehicle behavior.

3.1 Equation of Motion

The equations of motion of the model are derived from free-body diagrams of each component. A second order differential equation for each motion is obtained and these are given in Appendix I. Also included in Appendix I is a description of each vehicle parameter and its measured or calculated value. The equations are ordered and are of the form

$$\underset{7x7}{M}\ \underset{7x1}{\ddot{x}} + \underset{7x7}{H}\ \underset{7x1}{\dot{x}} + \underset{7x7}{K}\ \underset{7x1}{x} = \underset{7x1}{F}\ \underset{}{u} + \underset{7x1}{G}\ \underset{}{\dot{u}} \qquad (12)$$

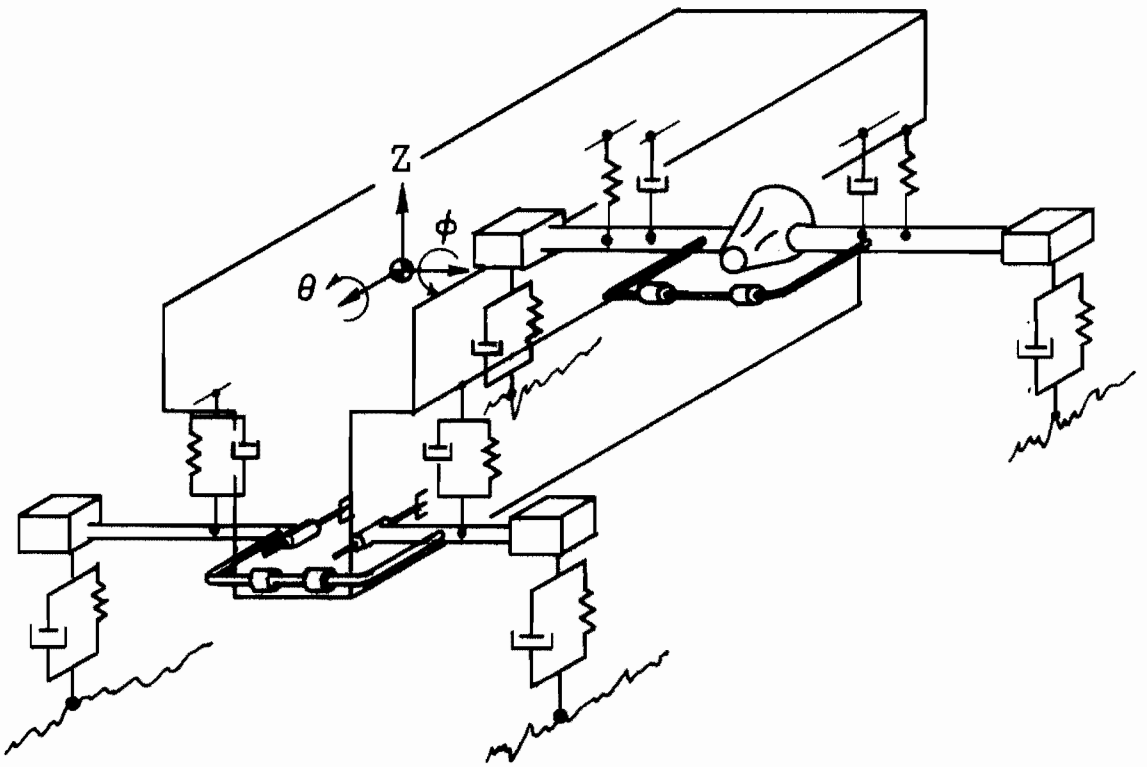

Figure 7. Diagram of Lumped Model of Automobile

The motion vector $\underline{x}$ =

$$\begin{bmatrix} \text{Sprung mass heave} \\ \text{Sprung mass pitch} \\ \text{Sprung mass roll} \\ \text{Rear axle hop} \\ \text{Rear axle roll} \\ \text{Left front wheel hop} \\ \text{Right front wheel hop} \end{bmatrix}$$

$\underline{F}$ relates to elevation inputs from the left and right wheel road tracks while $\underline{G}$ relates to the roadway inputs proportional to rate of change of roadway elevation.

$\underline{M}$ is a 7 x 7 mass matrix which is diagonal,

$\underline{H}$ is a 7 x 7 damping matrix which includes direct and cross-coupling terms and is not diagonal,

$\underline{K}$ is a 7 x 7 stiffness matrix including off diagonal cross-coupling terms.

Since $\underline{F}$ and $\underline{G}$ relate roadway elevation and evelation rate inputs to the front and rear suspensions they do not directly influence the rigid body motions and hence the upper 3 rows of $\underline{F}$ and $\underline{G}$ are all zero.

3.2 Solution Procedures for Vehicle Responses with Measured Road Data

The vehicle responds to elevation and elevation rate inputs which excite dynamic responses. The vehicle motion induces accelerations at passenger seating locations.

Because of the "stiff" nature of the vehicle dynamics, a Runge-Kutta integration procedure was discarded. Stability of the numerical algorithm is not guaranteed in these cases and generally a variable time step predictor-corrector routine is needed. The computer time is long.

Here, we choose to reduce equation 12 to first order form and take two different approaches. The first approach will reduce the vehicle equations to discrete time form under the assumption that the roadway is comprised of a series of step-like changes in elevation. The discretization distance for the step is

given by the speed of the profilometer divided by the sample rate whereas the discretization time for the vehicle equations is given by the discretization distance divided by the vehicle speed. Secondly, by reducing the vehicle model to four degrees of freedom (spring mass heave, pitch, front and rear wheel hops), the vehicle transfer functions will be found and, using equation 11, the power spectral density of the vehicle motions will be given for comparison.

Introducing by definition an additional vector

$$\underline{y} = \dot{\underline{x}} \tag{13}$$

equations 12 and 13 become

$$\begin{matrix} \dot{\underline{x}} \\ \dot{\underline{y}} \\ 14 \times 1 \end{matrix} = \begin{bmatrix} \underline{0} & \underline{I} \\ -\underline{M}^{-1}\underline{K} & -\underline{M}^{-1}\underline{H} \end{bmatrix} \begin{matrix} \underline{x} \\ \underline{y} \\ 14 \times 14 \end{matrix} + \begin{matrix} \begin{bmatrix} \underline{0} \\ \underline{M}^{-1}\underline{F} \end{bmatrix} \\ 14 \times 1 \end{matrix} \begin{matrix} \underline{u} \\ 14 \times 1 \end{matrix} + \begin{matrix} \begin{bmatrix} \underline{0} \\ \underline{M}^{-1}\underline{G} \end{bmatrix} \\ 14 \times 1 \end{matrix} \dot{\underline{u}} \tag{14}$$

And, by rearranging variables in the 14 x 1 state vector such that x_i and y_i are located in the new vector as $\hat{y}_i$ and $\hat{y}_{i+1}$, we arrive at the form

$$\begin{matrix} \dot{\hat{\underline{y}}} \\ 14x1 \end{matrix} = \begin{matrix} \underline{A} \\ 14x14 \end{matrix} \begin{matrix} \hat{\underline{y}} \\ 14x1 \end{matrix} + \begin{matrix} \underline{B} \\ 14x14 \end{matrix} \begin{matrix} \underline{u} \\ 14x1 \end{matrix} + \begin{matrix} \underline{C} \\ 14x14 \end{matrix} \begin{matrix} \dot{\underline{u}} \\ 14x1 \end{matrix} \tag{15}$$

with the vectors $\hat{\underline{y}}$ and $\underline{u}$ defined as

$$\hat{\underline{y}} = \begin{bmatrix} x_1 \\ \dot{x}_1 \\ x_2 \\ \dot{x}_2 \\ x_3 \\ \dot{x}_3 \\ x_4 \\ \dot{x}_4 \\ x_5 \\ \dot{x}_5 \\ x_6 \\ \dot{x}_6 \\ x_7 \\ \dot{x}_7 \end{bmatrix} \quad \text{and} \quad \underline{u} = \begin{bmatrix} \delta_1 \\ \delta_2 \\ \delta_3 \\ \delta_4 \end{bmatrix}$$

where x_1 through x_7 are as defined in (12), δ_1 and δ_2 are the roadway profiles under the left and right front tires respectively, and δ_3 and δ_4 are profiles under the left and right rear tires respectively. The elements A_{ij}, B_{ij}, and C_{ij} appear in Appendix I.

Equation (15) is rearranged to facilitate simulation by redefinition of the state vector as

$$\hat{\underline{x}} = (\hat{\underline{y}} - \underline{Cu})$$

to get

$$\dot{\hat{\underline{x}}} = \underline{A}\hat{\underline{x}} + (\underline{AC} + \underline{B})\,\underline{u} \tag{15b}$$

Using the zero order hold stepwise model for roadway elevation inputs $\underline{u}$, we have a sequence of inputs $\underline{u}_k$.
Solving (15b) in the interval t' to t' + Δt, where

$$\Delta t = \frac{\Delta s}{(\text{vehicle speed})}$$

is the discretization time,

$$\hat{\underline{x}}_{k+1} = \underline{P}\,\hat{\underline{x}}_k + \underline{Q}_1\underline{u}_k \;;\; \hat{\underline{x}}_0 = 0 \tag{16}$$

And

$$\underline{P} = \exp(\underline{A}\Delta t) = \underline{I} + \underline{A}\Delta t + \underline{A}^2\Delta t/_2^2 \ldots \underline{A}^N\,\Delta t^N_{N!} \quad .$$

$$\underline{Q} = (\underline{P} - \underline{I})(\underline{A}^{-1}\,\underline{B} + \underline{C}) \tag{17}$$

Equation 16 with $\underline{P}$ and $\underline{Q}$ defined as in equation 17 forms a recursive algorithm for updating values of the state vector $\hat{\underline{x}}_k$.

Motions of interest are contained in the elements of $\hat{\underline{x}}_k$ at each time point kΔt.

3.3 Acceleration Outputs

Of specific interest here are the acceleration values of passenger location points α_i:

$$\alpha_i = \underline{c}_i^T\,\dot{\hat{\underline{y}}} + \underline{d}_i^T\,\hat{\underline{y}} \tag{18}$$

where $\underline{c}_i$ is a conversion vector to translate accelerations about the vehicle CG to passenger locations and $\underline{d}_i$ is a conversion vector to resolve gravitational acceleration relative to the coordinate frame of the vehicle from pitch and roll rotations. The output acceleration can be found in terms of the state vector $\hat{\underline{x}}$ by substitution for $\underline{y}$ and $\dot{\underline{y}}$.

$$\alpha_i = \underline{c}_i^T (\dot{\hat{\underline{x}}} + \underline{C}\dot{\underline{u}}) + \underline{d}_i^T (\hat{\underline{x}} + \underline{C}\underline{u})$$

$$= \underline{c}_i^T \{\underline{A}\hat{\underline{x}} + (\underline{A}\underline{C} + \underline{B})\,\underline{u} + \underline{C}\dot{\underline{u}}\} + \underline{d}_i^T (\hat{\underline{x}} + \underline{C}\underline{u})$$

$$= (\underline{c}_i^T \underline{A} + \underline{d}_i^T)\,\hat{\underline{x}} + (\underline{c}_i^T \underline{A}\underline{C} + \underline{c}_i^T \underline{B} + \underline{d}_i^T \underline{C})\,\underline{u} + \underline{c}_i^T \underline{C}\,\dot{\underline{u}}$$

Noting that $\underline{c}_i^T \underline{B} = \underline{c}_i^T \underline{C} = \underline{d}_i^T \underline{C} = \underline{0}$, the above equation reduces to

$$\alpha_i = (\underline{c}_i^T \underline{A} + \underline{d}_i^T)\,\hat{\underline{x}} + \underline{c}_i^T \underline{A}\underline{C}\,\underline{u} \qquad (19a)$$

Thus an acceleration response sequance α_{ik} can be calculated directly from the state variable sequence $\hat{\underline{x}}_k$ and the input sequence $\underline{u}_k$ since

$$\alpha_{ik} = (\underline{c}_i^T \underline{A} + \underline{d}_i^T)\,\hat{\underline{x}}_k + \underline{c}_i^T \underline{A}\underline{C}\underline{u}_k \qquad (19b)$$

3.4 Summary

For each roadway profile under consideration the right and left wheel tracks give rise to a series of values for left side inputs to the vehicle δ_{1k} δ_{3k} and right side vehicle inputs δ_{2k} and δ_{4k} in which δ_3 is equal to δ_1 but delayed and where δ_4 is a delayed version of δ_2. Equation 16 gives the solution sequence for the state vector $\underline{x}_k$ at the time $k\Delta t$ corresponding to a $k\Delta s$ distance along the roadway. Equation 19 is used to convert the state vector into passenger point accelerations.

Care is taken to eliminate the initial points in the response sequence α_{ik} arising from the initial condition transient. Since it is difficult to estimate realistic initial conditions, the initial transient period was calculated but deleted from the subsequent power spectral data analysis. PSD computation was accomplished using the same procedure as for the roadway elevation power spectra. A typical profile and predicted acceleration response are shown in Figure 8.

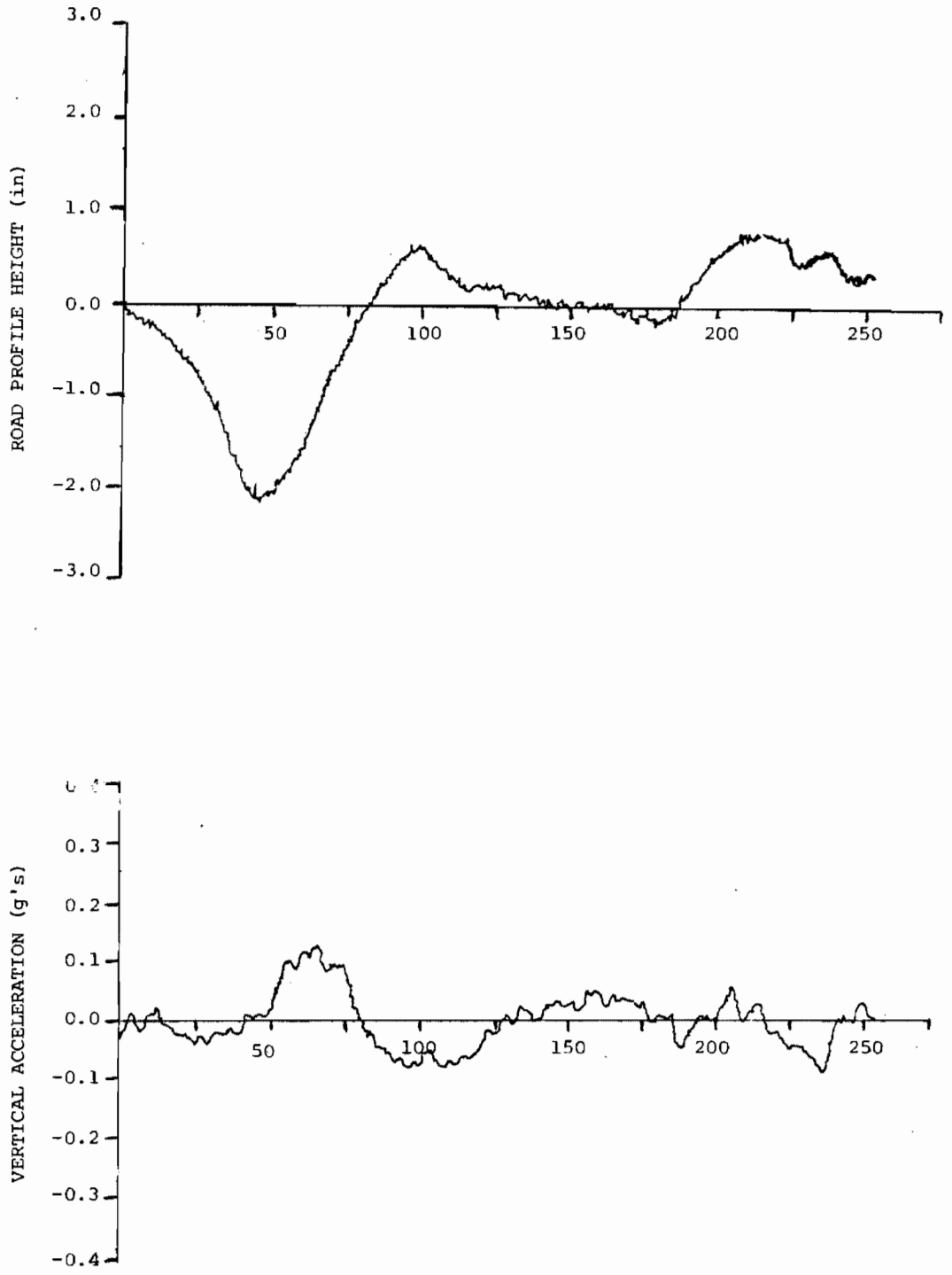

Figure 8. Typical Elevation Record and Corresponding CG Vertical Acceleration Response (THD Section 6)

3.5 Computation of Acceleration Power Spectra

The output acceleration sequence α_{ik} is now a sequence very similar to the digitized road profile data sequence and the power spectral density of the acceleration response is computed using the same procedures as outlined in equations 1-10.

3.6 Vehicle Transfer Functions for Reduced Model with A/f^2 Roadway Model

In view of the common use of four degree of freedom vehicle models with road profile statistics governed by equation 11, this section deals with the reduction of the model described previously to four degrees of freedom (eight state equations.) The roll modes of the spring mass and rear axle motion together with the hop mode of one of the two front wheels were eliminated from the model. This is necessary because of the lack of any general expression adequate to describe cross-power spectral properties between wheel tracks. The vehicle model can now be viewed as a block diagram, as shown in Figure 9. The transfer functions $G_1(j\omega)$ and $G_2(j\omega)$ can be calculated from the equations of the reduced model, and $e^{-j\omega T}$ represents the transit time delay between front and rear wheel contact points.

Rearranging the basic system equations and eliminating the variables associated with the modes being eliminated results in a new set of system dynamic equations:

$$\dot{\underline{r}} = \underline{A}_1 \underline{r} + \underline{B}_1 \underline{u} + \underline{C}_1 \dot{\underline{u}} \tag{20}$$

where $\underline{r}$ is a state vector

$$\underline{r} = \begin{bmatrix} z \\ \dot{z} \\ \phi \\ \dot{\phi} \\ r \\ v \\ \alpha_1 \\ s \end{bmatrix} \quad \text{and} \quad \underline{u} = \begin{bmatrix} \delta_1 \\ \delta_3 \end{bmatrix}$$

and the elements A_{1ij}, B_{1ij}, C_{1ij} are given in Appendix II.

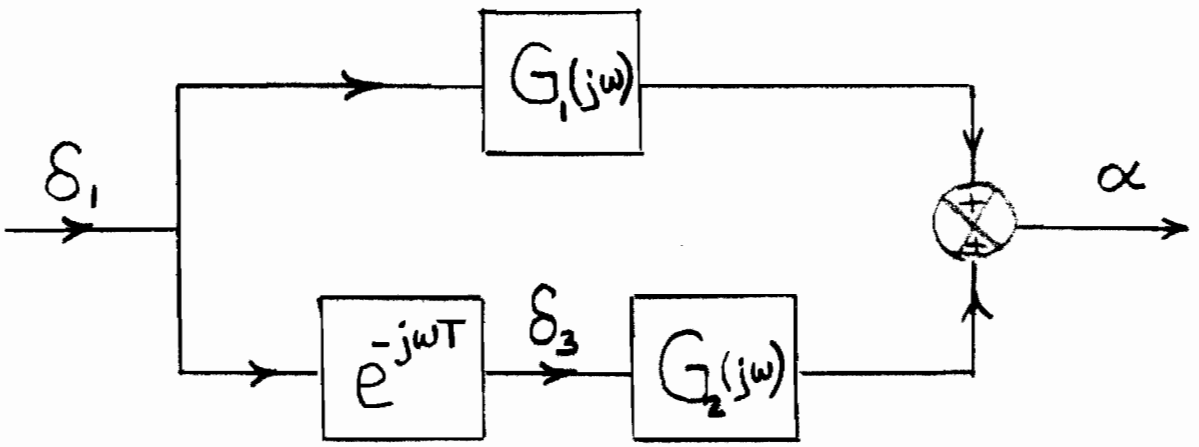

Figure 9. Block Diagram of Reduced Vehicle Model for Heave and Pitch Only

Employing complex notation for frequency response, the equations become

$$\underline{R} = (j\omega\underline{I} - \underline{A}_1)^{-1} \quad (\underline{B}_1 + j\omega\underline{C}_1)\ \underline{U} \tag{21}$$

and $$\alpha_i = j\omega \underline{c}_i^T\ \underline{R}$$

Equations can easily be rearranged as

$$\alpha_i = [\underline{c}_i^T(-\omega^2)(\underline{LB}_1 + \underline{A}_1\underline{LC}_1) + j\omega(\underline{A}_1\underline{LB}_1 - \omega^2\underline{LC}_1)]\ \underline{U} \tag{22}$$

where $$\underline{L} = (-\omega^2\underline{I} - \underline{A}_1^2)^{-1}$$

This form avoids the need to compute the inversion of the complex matrix

$$(j\omega\underline{I} - \underline{A}_1)^{-1}$$

Equation 22 will yield the real and imaginary parts of two transfer functions relating the influence of each input in $\underline{U}$ (i.e., δ_1 and δ_3) to the passenger point acceleration.

Thus $$\alpha_i = G_1(j\omega)\ \delta_1 + G_2(j\omega)\ \ \delta_2$$

where $$\omega^2 \underline{c}_i^T\ (\underline{LB}_1 + \underline{A}_1\underline{LC}_1) = [\mathrm{Re}(G_1);\ \mathrm{Re}(G_2)]$$

and $$\omega\underline{c}_i^T(\underline{A}_1\underline{LB}_1 - \omega^2\underline{LC}_1) = [\mathrm{Im}(G_1(j\omega));\ \mathrm{Im}(G_2(j\omega))]$$

Multiplying each value of $G_2(j\omega)$ by $e^{-j\omega\tau} = (\cos\omega\tau - j\sin\omega\tau)$ to effect the delay between front and rear contact points gives

$$G(j\omega) = G_1(j\omega) + e^{-j\omega\tau}\ G_2(j\omega)$$

as the overall transfer function between roadway profile

($|\delta_1| = |\delta_3|$) and passenger accelerations.

3.7 Power Density Spectrum of Reduced Model

With any linear system excited by a random input, the transfer function provides a simple relationship between the power density spectrum of the response and the power density spectrum (PSD) of the input. It is well known that

$$\text{PSD}\,\Big|_{\text{out}} = \text{PSD}\,\Big|_{\text{in}} \times (\text{amplitude of transfer function})^2$$

Thus if p(f) is the acceleration PSD and if

$$\text{PSD}_{\text{roadway}} = AV/_{f^2}\ \text{in}^2/\text{Hz}$$

then $$p(f) = \frac{AV}{f^2}\ \left| G(j2\pi f) \right|^2$$

Alternatively $$\frac{p(f)}{AV} = \frac{\left|G(j2\pi f)\right|^2}{f^2} \qquad (23)$$

Equation 23 is plotted in Figure 10 for the corresponding vehicle parameters as given in Appendix II.

A similar mathematical model has also developed the equivalent response for a vehicle in which only two degrees of freedom (four state variables) are considered viz. spring mass heave and wheel bounce. Now a single transfer function results and is substituted into (23) for comparison with the 8th order model as shown in Figure 10. Acceleration powers are found from Figure 10 by multiplication by an appropriate value of A chosen to provide a "best fit" to roadway profiles used later in the calculation of vehicle acceleration responses. Having employed logarithmic scales this is accomplished simply by a vertical shift of Figure 10 by the appropriate amount.

3.8 R.M.S. Values from Power Spectra

For a random process which is stationary and ergodic and has a zero mean there is a relationship between the mean square value and the power density spectrum. For a continuous signal, the mean square value $E(x^2)$ is given by

$$E(x^2) = \int_0^\infty p(f)df$$

where p(f) is the PSD function.

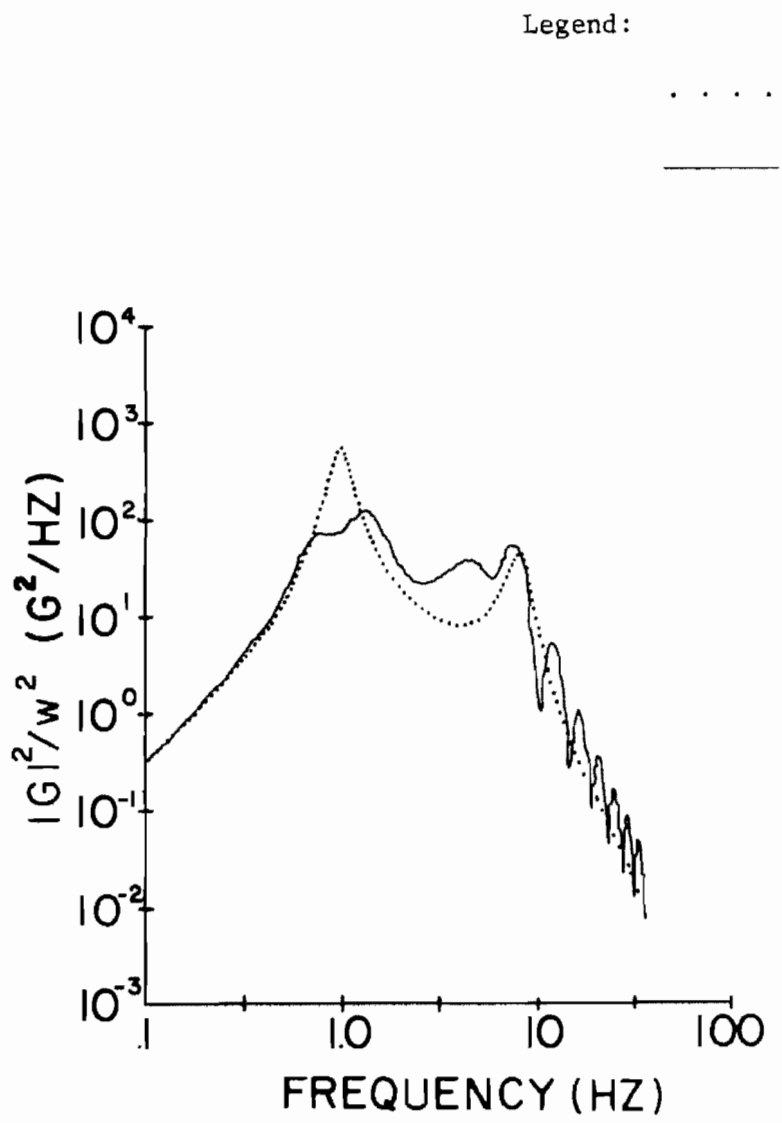

Figure 10. Plot of $|G(j2\pi f)|^2 \div f^2$ versus F : 8th Order Model and 4th Order Model

For a discretized signal of total time T given in terms of a sequence of N power density estimates $p_0 - - p_k - - p_{N-1}$

$$E(x^2) = \frac{1}{T} \sum_{k=0}^{N-1} p_k$$

The rms value of accelerations thus becomes

$$\alpha rms = \sqrt{\frac{1}{T} \sum_{k=0}^{N-1} p_k}$$

where p_k are values of acceleration power density.

Predicted rms acceleration will be given later for simulated rides over several measured test sections.

3.9 Comparison of Results

Three models of an automobile have been described; a fourth order model for body heave and wheel bounce motion; and eighth order model to include body pitch and independent front and rear wheel bounce motions and a fourteenth order model to include, additionally, body and rear axle roll modes.

Two different models for the roadway roughness have been considered. First, appropriate for the fourth and eighth order vehicle models only, single track random roughness with a power spectral density given by equation 11 is assumed. Its mean square value in the frequency range from 0.1 to 40.0 Hz is taken to be equal to that of later specified roadway sections. Second, a zero order hold model is used with random discretized inputs taken from actually measured roadway profiles. Here, either one or two tracks can be employed. The use of two tracks preserved the correct cross-correlation relationship between the two random inputs.

Figure 10 shows the comparison of fourth and eighth order models using equation 11 to describe the roughness. Clearly illustrated are the kinematic resonances occurring due to pitch mode excitation. Pitch mode contributions are apparent here because the passenger location is not at the vehicle's center of gravity. The results confirm that the lower order model produces essentially the same heave response peak at the low frequency (approximately 1 Hz.) as predicted by the eighth order model.

Figure 11 compares the effectiveness of an assumed roadway PSD according to equation 11 for predicting acceleration response power, with that obtained using measured profile inputs. The smooth characteristics of the reduced model results arise because of the smooth nature of the assumed roadway PSD. The measured roadway roughness gives rise to non-smooth data because of the finite sample length and nonstationarity of real roadways. The largest discrepancy shown by Figure 11 arises at low frequency because of the poor representation of roadway statistics by equation 11. Some of the scattering of the data in Figure 11 using measured roadway profiles could be eliminated through the choice of a longer test section. This, however, is difficult to accomplish practically for secondary roads, where straight sections of reasonable uniformity are hard to find.

Figure 12 compares the two reduced models with the fourteenth order model. Single track roughness profiles were used to excite the reduced models whereas the fourteenth order model employed two track inputs and roll motions were included in computing passenger location vertical acceleration. Figure 12 illustrates that the higher order models are necessary where effects of pitch and roll must be included. Even low frequency effects due to body heave motion are not well predicted by a fourth order vehicle model.

Figure 13 illustrates the differences in driver seat power when the two roadway tracks are taken to be identical (thus failing to excite roll motions in the vehicle) compared to the case using two different but measured tracks. Typically, the effects of roll induced by cross-correlation of the tracks results in up to 15% of the vertical rms acceleration at the driver's seat.

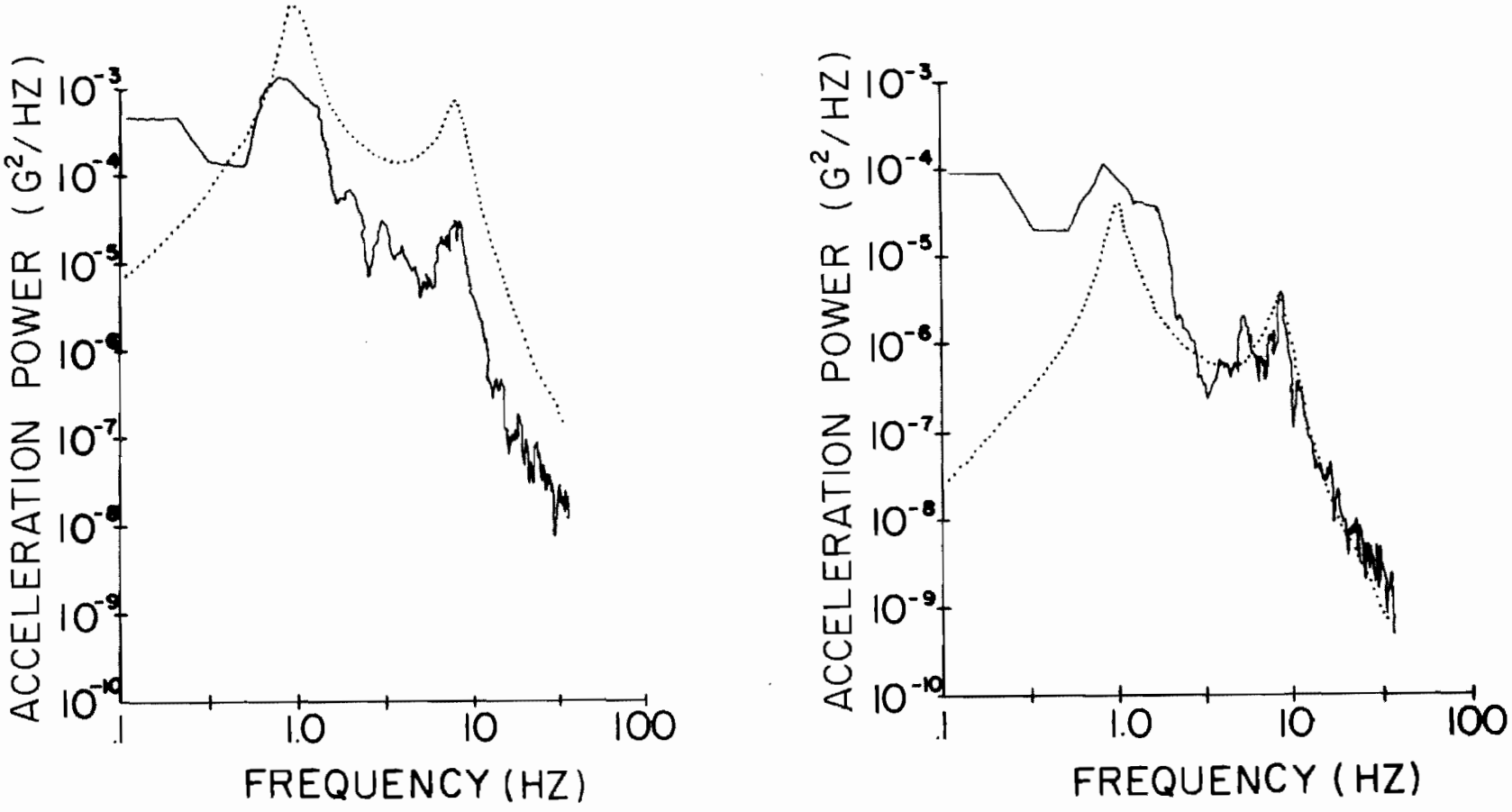

Figure 11. Comparison of Driver Seat Acceleration Power Using a Simple Roughness Model (A/F^2) with Measured Roughness Data and a Reduced 8th Order Vehicle Model

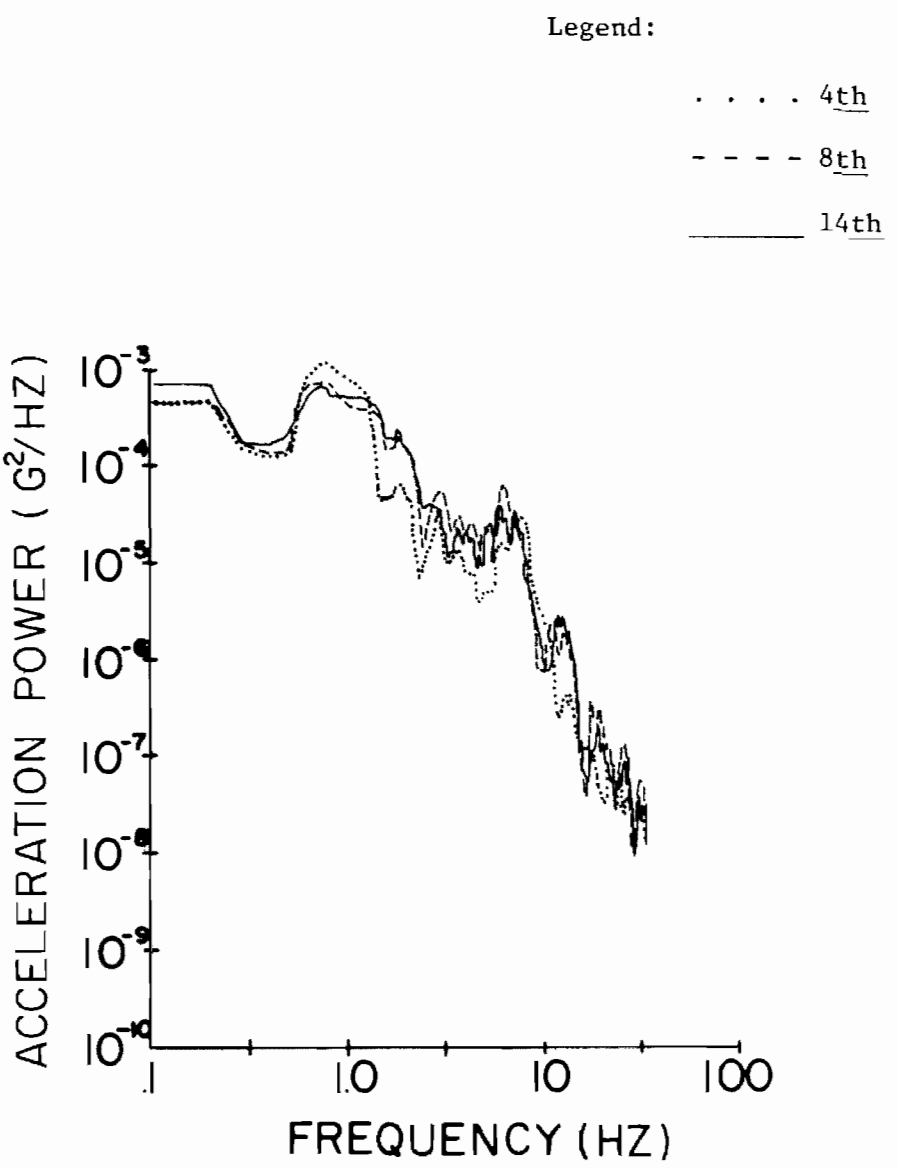

Figure 12. Comparison of Reduced Models of Vehicle and Roughness with 14th Order Model and Measured Roughness for Driver's Seat Acceleration Power Versus Frequency

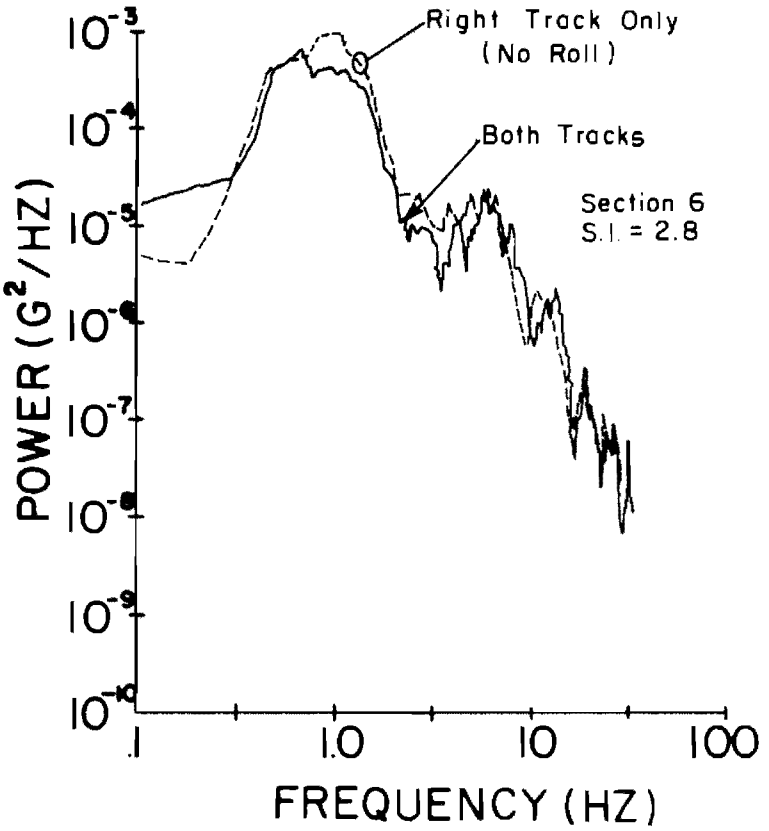

Figure 13. Effect of Cross-Correlation Between Tracks on Drivers Seat Acceleration Power

CHAPTER 4. ANALYSIS OF RIDE QUALITY

4.1 Roadway Servicability

Two different approaches to the automobile-highway system evaluation have developed over the past ten years or so. The first, from the highway engineer's viewpoint, is a measure of roadway servicability. This "servicability" concept, developed originally by Carey and Irick[19], had led most recently[20] to a predictive equation for a servicability index (S.I.). The S.I. value of a roadway is computed from an equation which operates on averaged roadway elevation power spectral estimates in defined wavelength bands. The constants in the equation are found through regression analysis to fit averaged subjective responses of a rating panel riding over several roadways in the test[21]. The S.I. value of a roadway is a scalar number within the range 0.0 to 5.0 which mimics the average subjective evaluation of that roadway section. S.I. is computed by the following:

$$\begin{aligned} S.I. = {} & 3.24 - 1.47X_1 - 0.133X_2 \\ & - 0.54X_3 + 1.08XC_1 - 0.25XC_2 \\ & + 0.08X_2X_3 - 0.91X_3X_4 + 0.67X_6X_{10} \\ & + 0.49T \end{aligned}$$

where

$$\begin{aligned} X_1 &= \log A_1 + 2.881 \\ X_2 &= \log A_2 + 4.065 \\ X_3 &= \log A_3 + 4.544 \\ X_4 &= \log A_4 + 4.811 \\ X_6 &= \log A_6 + 5.113 \\ X_{10} &= \log A_{10} + 5.467 \\ XC_1 &= \log C_1 + 3.053 \\ XC_5 &= \log C_5 + 5.659 \end{aligned}$$

and A_i is the average of the right and left wheel tracks (inches) centered at a special frequency of i x 0.023 cycle per foot.

---

[19] Ibid.

[20] Ibid.

[21] Roberts, F.L. and Hudson, W. R., "Pavement Servicability Equations Using the Surface Dynamics Profilometer," Research Report No. 73-3, Center for Highway Research, The University of Texas at Austin, 1970.

C_i is the average of the difference between right and left wheel tracks and T = 1 or 0 depending on whether the pavement is rigid or flexible respectively.

TABLE II.

Servicability Indices for Some of the Test Sections Employed

Section No.	SI Value
1	3.5
2	2.7
3	3.4
5	4.0
6	2.8
7	4.3

Table II gives values of servicability index for each of six sections which are part of those measured during this program. In view of the use of typical sedan automobiles in the experiments with road servicability, the servicability index should inherently represent a scalar measure of ride quality.

One of the drawbacks in the use of S.I. as a ride quality predictor is that vehicles with dynamic characteristics significantly different from those used in pavement rating studies fall outside the range of applicability. Including the effects of vehicle dynamics to predict passenger acceleration levels provides a calibration between accelerations and S.I. This calibration is explored in this section of the report.

In order to take into account the fact that human passengers are more sensitive to vibration frequency components in the 4-15 Hz range[22], a frequency weighted root mean square acceleration is also compared with roadway S.I. values. While much discrepancy exists between experimental test results for human subject response to vibration[23] some rationalization has recently been accomplished culminating in an International Standard[24]. The Standard is primarily useful for evaluating sinusoidal vibration although it is implied that narrow band filtered random vibrations may also be evaluated.

---

[22] Hanes, R.M., "Human Sensitivity to Whole Body Vibration," John Hopkins University, Applied Physics Laboratory Report TR -

[23] Ibid.

[24] "A Guide for the Evaluation of Human Exposure to Whole Body Vibration," International Standard 150/DIS 2631 International Organization for Standardization, New York, 1972.

The Standard 8 hour limit is reproduced in Figure 14.

Inverting this curve and normalizing over a frequency band a to b the frequency weighted rms accelerations are given by

$$(\text{wrmsg}) = \int_a^b W(f)\, p(f)\, df \qquad 1/2$$

where

$$W(f) = \frac{A^2(f)}{\frac{1}{(b-a)} \int_a^b A^2(f)\, df}$$

$A^2(f)$ is the squared inverse of the I.S.O. Standard of Figure 14 and W(f) is shown over the frequency range 0.1 - 40.0 Hz in Figure 15. It is necessary to use the squared values to preserve compatible units in the weighting function.

TABLE III.

Predicted rms Vertical Acceleration for Auto Parameters in Appendix I Both at the Vehicle C.G. and at the Driver's Seat

Section	rms Accel. (C.G.) (g's)	rms Accel. Driver's Seat (g's)
1	.0273	.0291
2	.0378	.0489
3	.0217	.0308
5	.0130	.0183
6	.0418	.0453
7	.0120	.0147

Table 3 and Figure 16 show a comparison between S.I. and predicted root mean square values of vehicle vertical acceleration. Both center of gravity accelerations and drivers seat accelerations are given. Both direct and frequency weighted rms values are given.

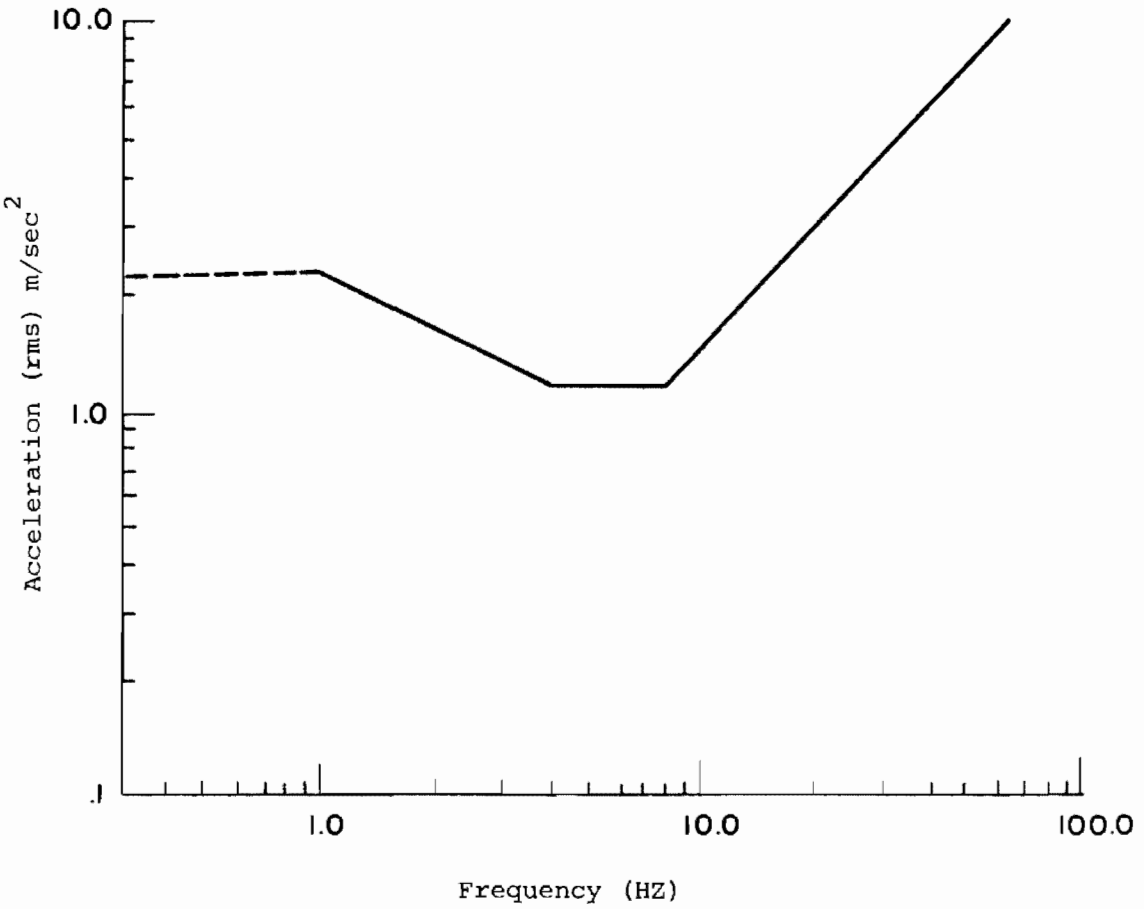

Figure 14. International Standard 8 Hour Limit

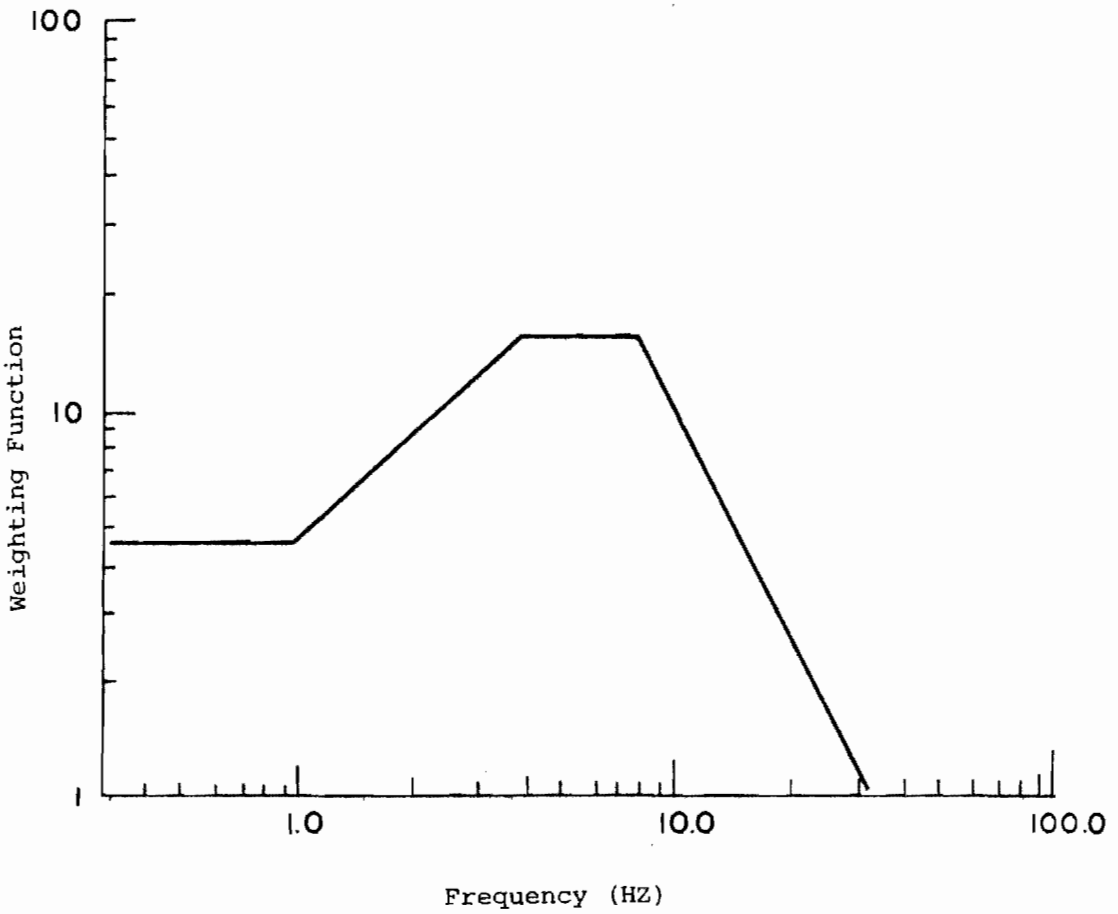

Figure 15. Weighting Function - Vertical Acceleration

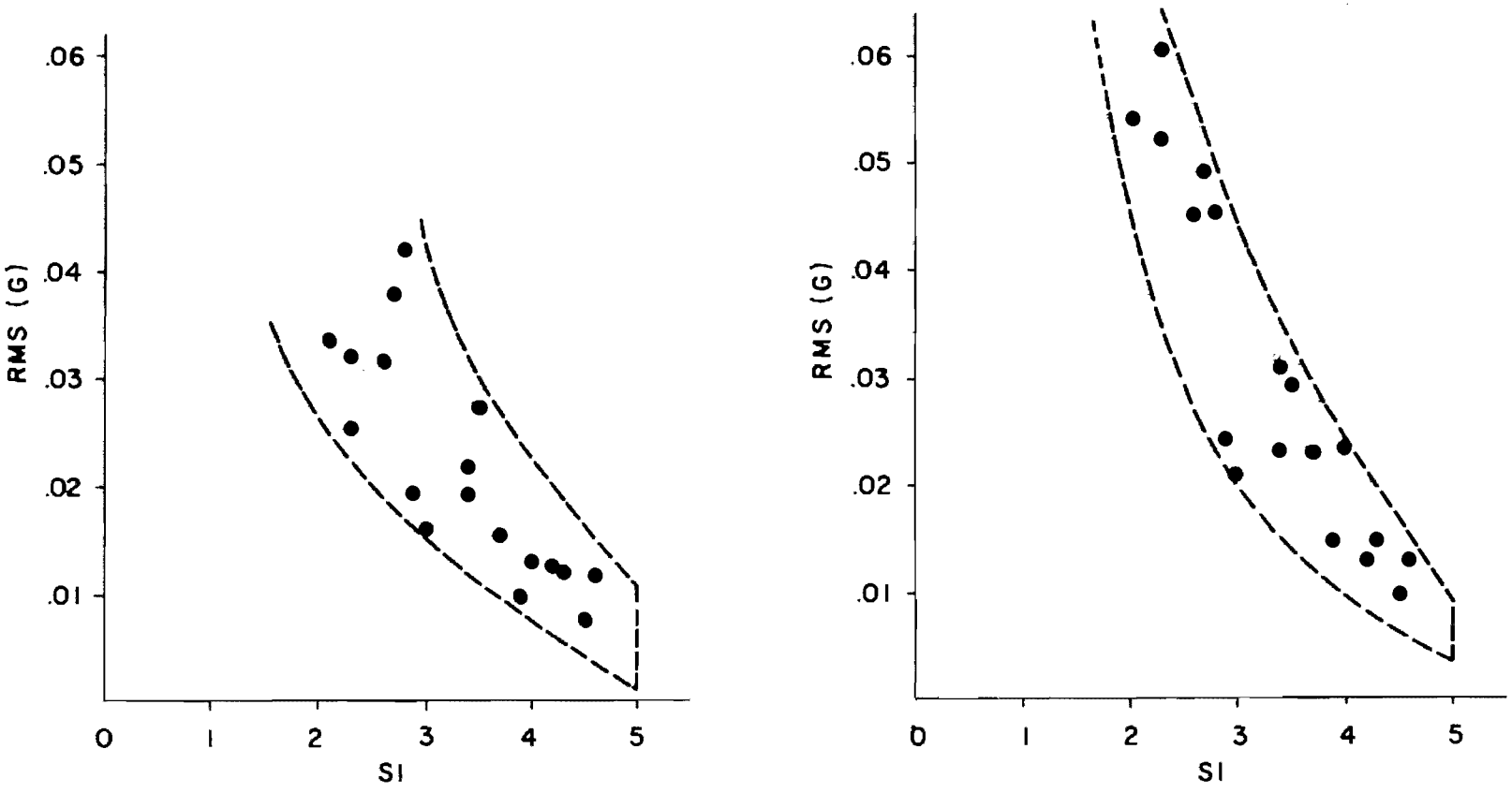

(a) Direct

Figure 16. Center for Gravity and Driver Seat Acceleration (rms) Versus Roadway SI

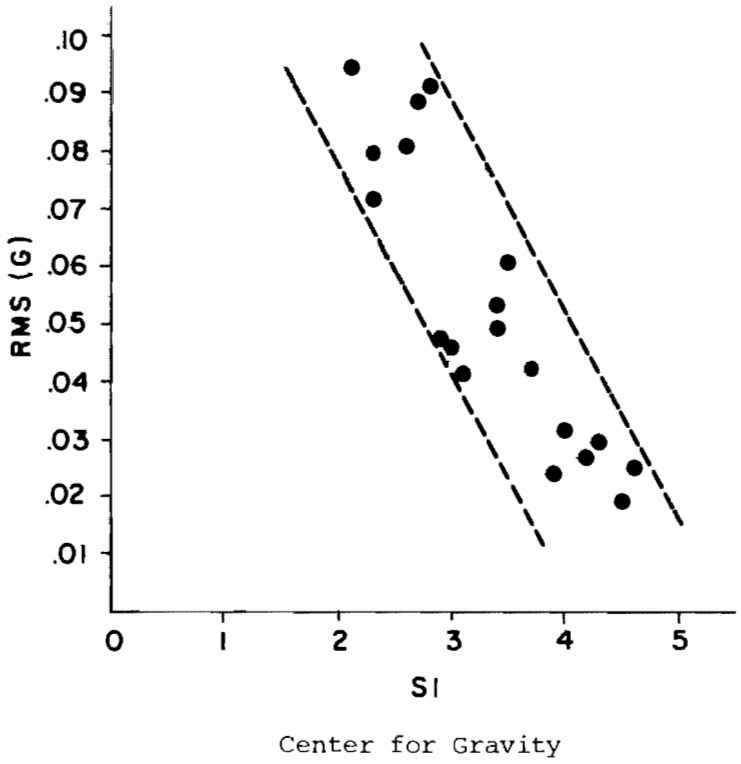

Center for Gravity

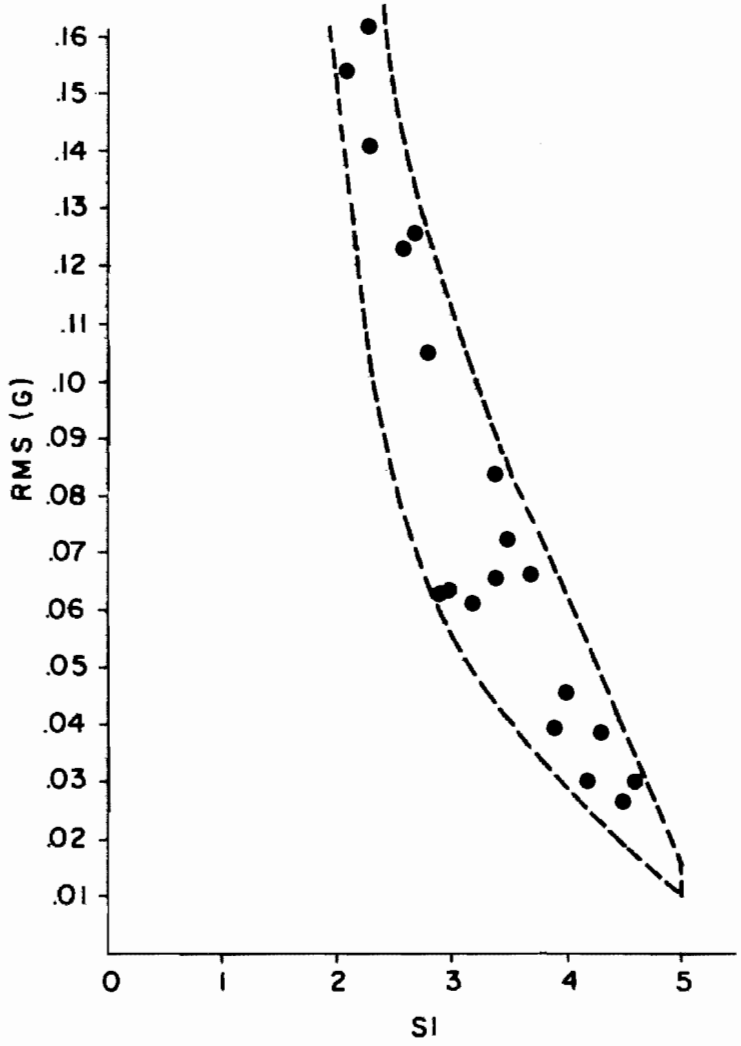

Driver Seat

(b) Frequency Weighted

Figure 16. (Continued)

Figure 16 illustrates that there is a direct correlation between acceleration levels and the roadway S.I. value. Also apparent is the improvement in correlation when frequency weighting is included. Passenger location point acceleration (rather than vehicle center of gravity acceleration) correlates better with S.I.

It would seem from Figure 16 that, for a smooth ride, frequency weighted driver seat acceleration should lie in the range of 0.0 - 0.05 g.

TABLE IV

	S.I. range	Frequency Weighted rmsg
Smooth ride	4.0 to 5.0	0.0 to 0.05
Medium ride	3.0 to 4.0	0.05 to 0.09
Rough ride	2.0 to 3.0	0.09 to 0.16

Table IV summarizes the comparison between rough, medium, and smooth conditions by range of S.I. for the roadway and range of frequency weighted root mean square accelerations.

4.2 Comparison of Acceleration Response with U.T.A.C.V. Specification

A specification for the allowed power spectral density composition of ride accelerations has recently been provided for the Urban Tracked Air-Chshion Vehicle Program[25] and is being used in design studies[26]. In Figure 17, predicted vertical acceleration PSD's are compared with the specifications. Six test sections were used and six predicted acceleration PSD's appear. The sections chosen vary in S.I. value from 2.7 to 4.3, covering the range of rough to smooth roadway. The smooth highway inputs produce acceleration PSD values significantly less than those given by the specifications and rough highway inputs give rise to values which also meet the specifications. The point here is that the

[25] Anon, "Design Specifications for the Urban Tracked Air-Cushion Vehicle," U.S. Dept. of Transportation, Washington, D.C., 1972.

[26] Hedrick, J.K., Billington, G.F., and Dresback, D.A., "Analysis, Design, and Optimization of High Speed Vehicle Suspensions Using State Variable Techniques," Preprints of 1974 Joint Automatic Control Conference, The University of Texas at Austin, June 19-20, 1974.

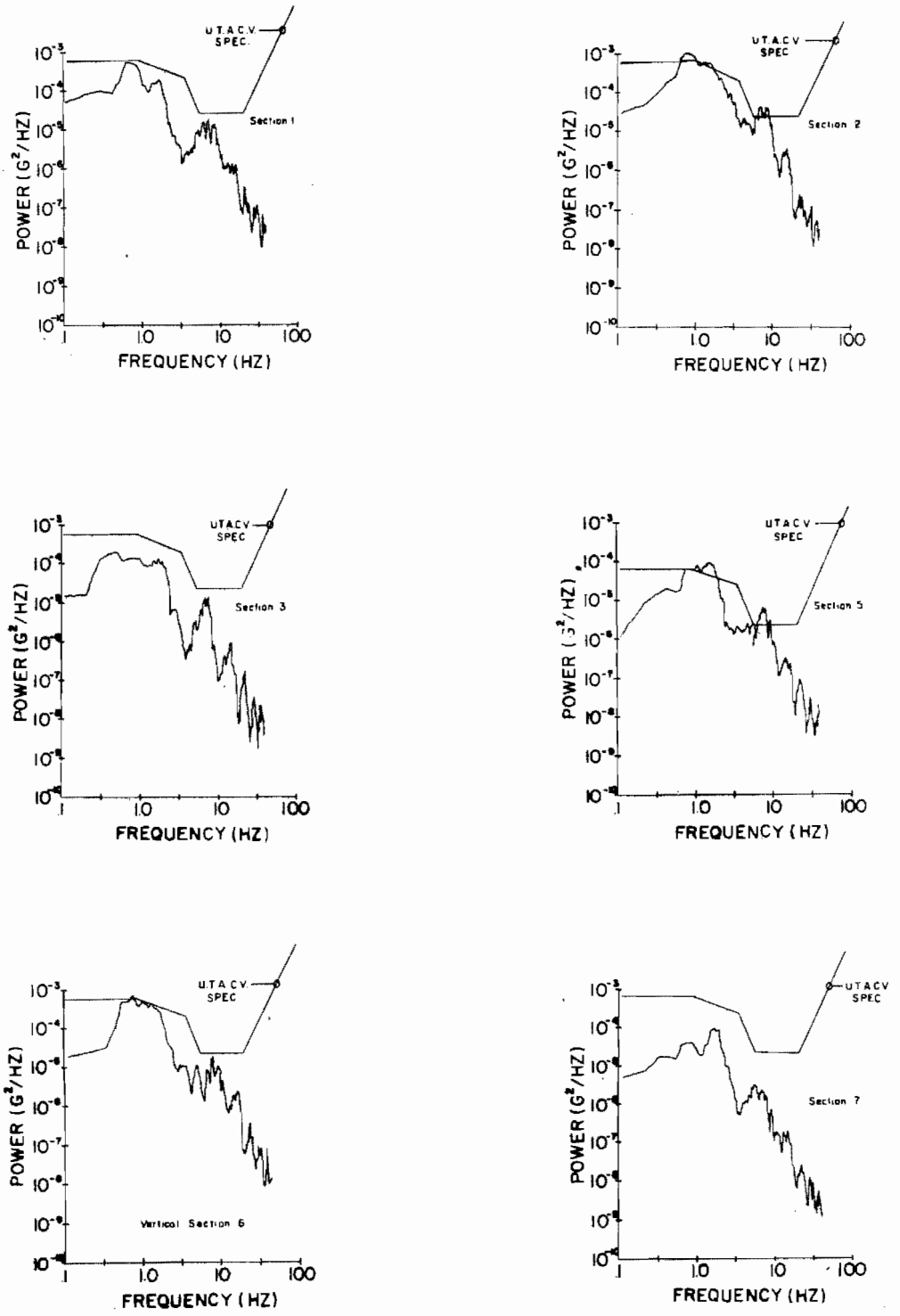

Figure 17. Predicted Driver's Seat Vertical Acceleration Power Compared with U.T.A.C.V. Specifications

specification would allow acceptable predicted acceleration levels with roadway inputs which are characterized as rough. If the vehicle model is reasonably representative of a real automobile in the frequency range of interest, one would conclude that the specifications are inadequate.

CHAPTER 5 CONCLUSIONS AND RECOMMENDATIONS

Resulting from this study of roadway roughness and vehicle modeling for random vibration response and its implication for ride quality, the following conclusions can be drawn.

1. The commonly assumed form for roadway random roughness power spectral density, that it is inversely proportional to the square of the spacial frequency, is not appropriate over the wavelengths of interest to ride quality for speeds around 50 mph. A better representation, possibly breaking the frequency range up into two or three bands, would be desirable.
2. Prediction of the vertical acceleration at passenger location points away from the vehicle body center of gravity will dictate the use of a fourteenth order vehicle model and roughness inputs for two tracks so that the body roll components can be included. Errors by neglecting roll motions account typically for up to 15% of the rms accelerations.
3. There is a relationship between rms acceleration and subjective response of riders as depicted by the roadway servicability index. (The servicability index is a measure of the roadway condition on a 0.0 to 5.0 scale).
4. Use of frequency weighted rms acceleration using the International Standard Constant Comfort Limits as a frequency weighting basis improves the correlation between rms acceleration and servicability index.
5. For good quality roadways with a servicability index in the 4.0 to 5.0 range, frequency weighted vertical accelerations should be below 0.05 wrmsg.

APPENDIX I

Vehicle Parameters and Equations of Motion

The equations of motions of the vehicle were derived by the summation of forces on free-body diagrams of the various vehicle subsystems, the front unsprung masses, the front lever arm, the front anti-sway bar, the rear axle, the rear anti-sway bar, and the body. Combining with constraint equations for the springs and dampers, the following seven-second order ordinary differential equations result.

Body Heave

$$M\ddot{Z} + (2(n_s/n_t)^2 C_F + 2C_R) Z + (2(n_s/n)^2 K_{SF} + 2K_{SR}) - (2(n_s/n_t)^2 X_{FS} C_F - 2 X_{RC} C_R)\dot{\Phi} - (2(n_s/n_t) X_{FS} K_{SF} - ZK_{SR} X_{RS})\Phi - 2K_{SR}\zeta - 2C_R\dot{\zeta} - (n_s/n_t)^2 K_{SF} a_1 - (n_s/n_t)^2 \dot{a}_1 - (n_s/n_t)^2 K_{SF} a_2 - (n_s/n_t)^2 C_F \dot{a}_2 = 0$$

Body Roll

$$I_{sx}\ddot{\theta} + [2C_F(Y_{FS} - B_F(1-n_s/n_t))^2 + 2 C_R Y_{RC}^2]\dot{\theta} + [2K_{SF}(Y_{FS} - B_F(1-n_s/n_t))^2 + 4 K_{FB}/R_F (n_B + B_F n_B/n_t)^2 + 2Y_{RS}^2 K_{SR} + 4 K_{RB}/R_R B_B^2]\theta - (2K_{SR} Y_{RS} B_S + 4 K_{RB}/R_R B_B^2)\xi - 2C_R Y_{RC} B_C \dot{\xi} - [K_{SF}(Y_{FS} - B_F(1-n_s/n_t)) n_s/n_t + 2 K_{FB}/R_F (n_B + B_F n_B/n_t) n_B/n_t] a_1 - C_F (Y_{FS} - B_F(1-n_s/n_t)) n_s/n_t \dot{a}_1 + [K_{SF}(Y_{FS} - B_F(1-n_s/n_t)) n_s/n_t + 2 K_{FB}/R_F (n_B + B_F n_B/n_t) n_B/n_t] a_2 + C_F (Y_{FS} - B_F (1-n_s/n_t)) n_s/n_t \dot{a}_2 = 0$$

Body Pitch

$$I_{SY}\ddot{\Phi} - 2((n_s/n_t)^2 K_{SF} X_{FS} - K_{SR} X_{RS}) Z - 2 (n_s/n_t)^2 C_F X_{FS} C_R X_{RC}) \dot{Z} + 2((n_s/n_t)^2 K_{SF} X_{FS}^2 + K_{SR} X_{RS}^2)\Phi + 2(((n_s/n_t)^2 C_F X_{FS}^2 + C_R X_{RC}^2)\dot{\Phi} - 2 K_{SR} X_{RS}\zeta - 2 C_R X_{RC}\dot{\zeta} + (n_s/n_t)^2 K_{SF} X_{FS} a_1 + (n_s/n_t)^2 C_F X_{FS} \dot{a}_1 + (n_s/n_t)^2 K_{SF} X_{FS} a_2 + (n_s/n_t)^2 C_F X_{FS} \dot{a}_2 = 0$$

Rear Axle Heave

$$M_{RU}\ddot{\zeta} - 2K_{RS}\,Z - 2C_R\,\dot{z} - 2\,K_{SR}\,X_{RS}\Phi - 2\,C_R\,X_{RC}\dot{\Phi}$$

$$+ 2(K_{SR}+K_{TR})\zeta + 2(C_R + C_{TR})\dot{\zeta} = K_{TR}(\delta_3+\delta_4) + C_{TR}(\dot{\delta}_3+\dot{\delta}_4)$$

Rear Axle Roll

$$I_{RU}\ddot{\xi} - (2B_sY_{RS}K_{SR} + 4\,B_B{}^2K_{RB}/R_R)\theta - 2\,B_C\,Y_{RC}\,C_R\dot{\theta}$$

$$+(2B_T^2\,K_{TR} + 2\,B_S^2\,K_{SR} + 2\,B_S^2\,K_{SR} + 4\,B_B^2\,K_{RB}/R_R)\xi$$

$$+(2B_T^2\,C_{TR} + 2B_C^2\,C_R)\dot{\xi} = B_T\,K_{TR}\,(\delta_3-\delta_4) + B_T\,C_{TR}(\dot{\delta}_3-\dot{\delta}_4)$$

Left/Right Front Wheels Motion

$$M_{UF}\begin{bmatrix}\ddot{a}_1\\ \ddot{a}_2\end{bmatrix} - (n_s/n_t)^2K_{SF}\,Z - (n_s/n_t)^2C_F\,\dot{Z} + (n_s/n_tK_{SF}((1-n_s/n_t)B_F$$

$$-Y_{FS}) -2(n_s/n_t)\,(K_{FB}/R_F)(n_B/n_t\,B_F + n_B))\theta + n_s/n_tC_F((1-n_s/n_t)$$

$$B_F - Y_{FS})\dot{\theta} + (n_s/n_t)\,K_{SF}X_{FS}\Phi + (n_s/n_t)^2\,C_F\,X_{FS}\dot{\Phi} + (K_{TF} +$$

$$(n_s/n_t)^2\,K_{SF} + (n_s/n_t)^2\,K_{FB}/R_R)\begin{bmatrix}a_1\\ a_2\end{bmatrix} + (C_{TF} + n_s/n_t)^2$$

$$C_F)\begin{bmatrix}\dot{a}_1\\ \dot{a}_2\end{bmatrix} - (n_B/n_t)^2\,K_{FB}/R_F\begin{bmatrix}a_2\\ a_1\end{bmatrix} = K_{TF}\begin{Bmatrix}\delta_1\\ \delta_2\end{Bmatrix} + C_{TF}\begin{Bmatrix}\dot{\delta}_1\\ \dot{\delta}_2\end{Bmatrix}$$

VALUE OF DISTANCES

FOR 1974 BUICK CENTURY

XFS = 43.0	in	NS = 10.0	in
XRS = 73.5	in	NC = 10.0	in
XRC = 73.5	in	NB = 15.0	in
YFS = 18.75	in	BT = 30.75	in
YFB = 15.75	in	BS = 17.75	in
YRS = 17.5	in	BC = 19.00	in
YRC = 17.0	in	BB = 0.0	in
YRB = 0.0	in	RF = 11.0	in
BF = 15.75	in	RR = 0.0	in
NT = 17.0	in		

VALUES OF MASSES AND INERTIA FOR 1974 BUICK CENTURY

MS =	9.8	lb-sec/in
MRU =	1.0	lb-sec/in
MUF =	.3	lb-sec/in
ISX =	5640.	$in\text{-}lb\text{-}sec^2$
ISY =	31500.	$in\text{-}lb\text{-}sec^2$
IRU =	400.0	$in\text{-}lb\text{-}sec^2$

STIFFNESS AND DAMPING CHARACTERISTICS
FOR AN 1974 BUICK CENTURY

KSF =	220 lb/in	CF =	18.02 lb-sec/in
KSR =	160 lb/in	CR =	12.01 lb-sec/in
KTF =	1150 lb/in	CTF =	1.0 lb-sec/in
KTR =	1150 lb/in	CTR =	1.0 lb-sec/in
KFB =	2400 in-lb/rad		
KRB =	0.0 in-lb/rad		

$$
A = \begin{bmatrix}
0 & 1 & 0 & 0 & 0 & 0 & 0 & 0 & 0 & 0 & 0 & 0 & 0 & 0 \\
-2F3/MS & -2F1/MS & 0 & 0 & 2F4/MS & 2F2/MS & 2K_{SR}/MS & 2C_R/MS & 0 & 0 & MKS/MS & MCC/MS & MKS/MS & MCC/MS \\
0 & 0 & 0 & 1 & 0 & 0 & 0 & 0 & 0 & 0 & 0 & 0 & 0 & 0 \\
0 & 0 & -2F6/ISX & -2F6/ISX & 0 & 0 & 0 & 0 & 2F7/ISX & \frac{2B_C Y_{RB} C_R}{ISX} & F8/ISX & F19/ISX & -F8/ISX & -F19/ISX \\
0 & 0 & 0 & 0 & 0 & 1 & 0 & 0 & 0 & 0 & 0 & 0 & 0 & 0 \\
2F4/ISY & 2F2/ISY & 0 & 0 & -F10/ISY & -2F9/ISY & \frac{2X_{RS}K_{SR}}{ISY} & \frac{2X_{RC}C_R}{ISY} & 0 & 0 & -\frac{X_{FS}MKS}{ISY} & -\frac{X_{FS}MCC}{ISY} & -\frac{X_{FS}MKS}{ISY} & -\frac{X_{FS}MCC}{ISY} \\
0 & 0 & 0 & 0 & 0 & 0 & 0 & 1 & 0 & 0 & 0 & 0 & 0 & 0 \\
2K_{SR}/MRU & 2C_R/MRU & 0 & 0 & \frac{2X_{RS}K_{SR}}{MRU} & \frac{2X_{RC}C_R}{MRU} & -2F12/MRU & -2F11/MRU & 0 & 0 & 0 & 0 & 0 & 0 \\
0 & 0 & 0 & 0 & 0 & 0 & 0 & 0 & 0 & 1 & 0 & 0 & 0 & 0 \\
0 & 0 & 2F14/IRU & \frac{2B_C Y_{RC} C_R}{IRU} & 0 & 0 & 0 & 0 & -2F14/IRU & -2F13/IRU & 0 & 0 & 0 & 0 \\
0 & 0 & 0 & 0 & 0 & 0 & 0 & 0 & 0 & 0 & 0 & 1 & 0 & 0 \\
MKS/MUF & MCC/MUF & F17/MUF & F15/MUF & -\frac{X_{FS}MKS}{MUF} & -\frac{X_{FS}MCC}{MUF} & 0 & 0 & 0 & 0 & -F18/MUF & -F16/MUF & F20/MUF & 0 \\
0 & 0 & 0 & 0 & 0 & 0 & 0 & 0 & 0 & 0 & 0 & 0 & 0 & 1 \\
MKS/MUF & MCC/MUF & -F17/MUF & -F15/MUF & -\frac{X_{FS}MKS}{MUF} & -\frac{X_{FS}MCC}{MUF} & 0 & 0 & 0 & 0 & F20/MUF & -F18/MUF & -F16/MUF & 0
\end{bmatrix}
$$

$$B = \begin{bmatrix} & & \begin{bmatrix} 0 \\ 7x4 \end{bmatrix} & \\ 0 & 0 & 0 & 0 \\ 0 & 0 & K_{TR}/M_{RU} & K_{TR}/M_{RU} \\ 0 & 0 & 0 & 0 \\ 0 & 0 & K_{TR}*BT/I_{RU} & -K_{TR}*B_T/I_{RU} \\ 0 & 0 & 0 & 0 \\ K_{TF}/M_{UF} & 0 & 0 & 0 \\ 0 & K_{TF}/M_{UF} & 0 & 0 \end{bmatrix}$$

$$C = \begin{bmatrix} & & \begin{bmatrix} 0 \\ 7x4 \end{bmatrix} & \\ 0 & 0 & 0 & 0 \\ 0 & 0 & C_{TR}/M_{RU} & C_{TR}/M_{RU} \\ 0 & 0 & 0 & 0 \\ 0 & 0 & C_{TR}*B_T/I_{RU} & -C_{TR}*B_T/I_{RU} \\ 0 & 0 & 0 & 0 \\ C_{TF}/M_{UF} & 0 & 0 & 0 \\ 0 & C_{TF}/M_{UF} & 0 & 0 \end{bmatrix}$$

APPENDIX II

$$A_1 = \begin{bmatrix} 0 & 1 & 0 & 0 & 0 & 0 & 0 & 0 \\ \frac{-2F3}{MS} & \frac{-2F1}{MS} & \frac{2F4}{MS} & \frac{2F2}{MS} & \frac{2K_{SR}}{MS} & \frac{2C_R}{MS} & \frac{2NKS}{MS} & \frac{2NCC}{MS} \\ 0 & 0 & 0 & 1 & 0 & 0 & 0 & 0 \\ \frac{2F4}{ISY} & \frac{2F2}{ISY} & \frac{-2F10}{ISY} & \frac{-2F9}{ISY} & \frac{2X_{RS}K_{SR}}{ISY} & \frac{2X_{RC}C_R}{ISY} & \frac{-(NKS)X_{FS}}{ISY} & \frac{-(NCC)X_{FS}}{ISY} \\ 0 & 0 & 0 & 0 & 0 & 1 & 0 & 0 \\ \frac{2K_{SR}}{MRU} & \frac{2C_R}{MRU} & \frac{2X_{RS}K_{SR}}{MRU} & \frac{2X_{RS}K_{SR}}{MRU} & \frac{-2F12}{MRU} & \frac{-2F11}{MRU} & 0 & 0 \\ 0 & 0 & 0 & 0 & 0 & 0 & 0 & 1 \\ \frac{2NKS}{MUF} & \frac{2NCC}{MUF} & \frac{-2X_{FS}NKS}{MUF} & \frac{-2X_{FS}NCC}{MUF} & \frac{-2F20}{MUF} & \frac{-2F18}{MUF} & \frac{-2F16}{MUF} & 0 \end{bmatrix}$$

$$B_1 = \begin{bmatrix} 0 & 0 \\ 0 & 0 \\ 0 & 0 \\ 0 & 0 \\ 0 & 0 \\ 0 & 2K_{TR}/MRU \\ 0 & 0 \\ 2K_{TF}/MUF & 0 \end{bmatrix} \qquad C_1 = \begin{bmatrix} 0 & 0 \\ 0 & 0 \\ 0 & 0 \\ 0 & 0 \\ 0 & 0 \\ 0 & 2C_{TR/MRU} \\ 0 & 0 \\ 2C_{TF/MUF} & 0 \end{bmatrix}$$

RESEARCH MEMORANDA PUBLISHED BY THE COUNCIL FOR ADVANCED TRANSPORTATION STUDIES

1 *Human Response in the Evaluation of Modal Choice Decisions.* C. Shane Davies, Mark Alpert, and W. Ronald Hudson, April 1973.

2 *Access to Essential Services.* Ronald Briggs, Charlotte Clark, James Fitzsimmons, and Paul Jensen, April 1973.

3 *Psychological and Physiological Responses to Stimulation.* D. W. Wooldridge, A. J. Healey, and R. O. Stearman, August 1973.

4 *An Intermodal Transportation System for the Southwest: A Preliminary Proposal.* Charles P. Zlatkovich, September 1973.

5 *Passenger Travel Patterns and Mode Selection.* Shane Davies, Mark Alpert, Harry Wolfe, and Rebecca Gonzalez, October 1973.

6 *Segmenting a Transportation Market by Determinant Attributes of Modal Choice.* Shane Davies and Mark Alpert, October 1973.

7 *The Interstate Rail System: A Proposal.* Charles P. Zlatkovich, December 1973.

8 *Literature Survey on Passenger and Seat Modeling for the Evaluation of Ride Quality.* Bruce Shanahan, Ronald Stearman, and Anthony Healey, November, 1973.

9 *The Definition of Essential Services and the Identification of Key Problem Areas.* Ronald Briggs and James Fitzsimmons, January, 1974.

10 *A Procedure for Calculating Great Circle Distances Between Geographic Locations.* J. Bryan Adair, March 1974.

11 *MAPRINT: A Computer Program for Analyzing Changing Locations of Non-Residential Activities.* Graham Hunter, Richard Dodge, and C. Michael Walton, March 1974.

12 *A Method for Assessing the Impact of the Energy Crisis on Highway Accidents in Texas.* E. L. Frome and C. Michael Walton, February 1975.

13 *State Regulation of Air Transportation in Texas.* Robert C. Means and Barry Chasnoff, April 1974.

14 *Transportation Atlas of the Southwest.* Charles P. Zlatkovich, S. Michael Dildine, Eugene Robinson, James W. Wilson, and J. Bryan Adair, June 1974.

15 *Local Government Decisions and Land-Use Change: An Introductory Bibliography.* W. D. Chipman, May 1974.

16 *An Analysis of the Truck Inventory and Use Survey Data for the West South Central States.* Michael Dildine, July 1974.

17 *Towards Estimating the Impact of the Dallas-Fort Worth Regional Airport on Ground Transportation.* William J. Dunlay and Lyndon Henry, September 1974.

18 *The Attainment of Riding Comfort for a Tracked Air-Cushion Vehicle Through the Use of an Active Aerodynamic Suspension.* Bruce Shanahan, Ronald Stearman, and Anthony Healey, September 1974.

19 *Legal Obstacles to the Use of Texas School Buses for Public Transportation.* Robert Means, Ronald Briggs, John E. Nelson, and Alan J. Thiemann, January 1975.

20 *Pupil Transportation: A Cost Analysis and Predictive Model.* Ronald Briggs and David Venhuizen, April 1975.

21 *Variables in Rural Plant Location: A Case Study of Sealy, Texas.* Ronald Linehan, C. Michael Walton, and Richard Dodge, February 1975.

22 *A Description of the Application of Factor Analysis to Land Use Change in Metropolitan Areas.* John Sparks, Carl Gregory, and Jose Montemayor, December 1974.

23 *A Forecast of Air Cargo Originations in Texas to 1990.* Mary Lee Metzger Gorse, November 1974.

24 *A Systems Analysis Procedure for Estimating the Capacity of an Airport: A Selected Bibliography.* Chang-Ho Park, Edward V. Chambers III, and William J. Dunlay, Jr., August 1975.

25 *System 2000—Data Management for Transportation Impact Studies.* Gordon Derr, Richard Dodge and C. Michael Walton, September 1975.

26 *Regional and Community Transportation Planning Issues—A Selected Bibliography.* John Huddleston, Ronald Linehan, Abdulla Sayyari, Richard Dodge, C. Michael Walton, and Marsha Hamby, September 1975.

27 *A Systems Analysis Procedure for Estimating the Capacity of an Airport: System Definition, Capacity Definition, and Review of Available Models.* Edward V. Chambers III, Tommy Chmores, William J. Dunlay, Jr., Nicolau D. F. Gualda, B. F. McCullough, Chang-Ho Park, and John Zaniewski, October 1975.

28 *The Application of Factor Analysis to Land Use Change in a Metropolitan Area.* John Sparks and Jose Montemayor, November 1975.

29 *Current Status of Motor Vehicle Inspection: A Survey of Available Literature and Information.* John Walter Ehrfurth and David A. Sands, December 1975.

30 *Executive Summary: Short Range Transit Improvement Study for The University of Texas at Austin.* C. Michael Walton (Supervising Professor), May 1976.

Council for Advanced Transportation Studies

THE UNIVERSITY OF TEXAS AT AUSTIN